METAL SPECIATION'S ROLE IN TOXICITY, BIOAVAILABILITY, AND BIO-REACTIVITY IN THE RAINBOW TROUT (*ONCORHYNCHUS MYKISS*) GUT CELL LINE (RTgutGC)

By

DEAN OLDHAM

Bachelor of Science in Integrative Biology

Oklahoma State University

Stillwater, Oklahoma

2018

Submitted to the faculty of the Graduate College of
Oklahoma State University
in partial fulfillment of
the requirements for
the Degree of
MASTER OF SCIENCE
December 2020

METAL SPECIATION'S ROLE IN TOXICITY, BIOAVAILABILITY, AND BIO-REACTIVITY IN THE RAINBOW TROUT (ONCORHYNCHUS MYKISS) GUT CELL LINE (RTGUTGC)

Thesis Approved:

Matteo Minghetti

Thesis Adviser

Jason Belden

Scott McMurry

ACKNOWLEDGEMENTS

I would like to thank my advisor Matteo Minghetti for allowing me the opportunity of working in his lab during my undergraduate degree and accepting me for master's research. My abilities as a scientist are due to his guidance and a simple "thank you" isn't enough to show my gratitude.

I would also like to thank my committee members Scott McMurry and Jason Belden for their work in peer reviewing this thesis, as well as their advice on testing, methodology, and different data analysis to explore.

A large thank you to all of my lab mates Md Ibrahim, Justin Scott, and Debarati Chanda who helped me through this research with their past experience and their help with data collection.

Thank you to the Oklahoma State University Interdisciplinary Toxicology Fellowship Program for additional monetary assistance with my research.

Lastly, and most importantly, I would like to thank my wife, Brendyn, and two children, Kevine and James. Without them and their relentless support, I would not be here today. I would not have been able to make it through my busy and stressful nights, weekends, and time crunches without you.

Name: DEAN OLDHAM

Date of Degree: DECEMBER 2020

Title of Study: METAL SPECIATION'S ROLE IN TOXICITY, BIOAVAILABILITY, AND BIO-REACTIVITY IN THE RAINBOW TROUT (ONCORHYNCHUS MYKISS) GUT CELL LINE (RTGUTGC)

Major Field: INTEGRATIVE BIOLOGY

Abstract: The bioavailability of metal complexes is poorly understood. To evaluate the bioavailability and toxicity of neutral, and charged metal complexes, as well as free metal ions, Visual Minteq, a chemical equilibrium model, was used to design different exposure media to allow the formation of a variety of metal species. Two non-essential (silver and cadmium) and two essential (copper and zinc) metals were selected. The rainbow trout (*Oncorhynchus mykiss*) gut cell line (RTgutGC) was used to investigate the bioavailability, bioreactivity and toxicity of different metal species. Dose response curves were calculated using a multiple endpoint cytotoxicity assay which measures simultaneously metabolic activity, cell membrane and lysosomal integrity. Bioavailability of different metal species was evaluated by exposing cells to an identical non-toxic dose of metal. Intracellular metal was then measured by ICP-MS. Bioreactivity was measured by quantification of mRNA levels of genes that respond to metal toxicity, such as metallothionein (MT), oxidative stress such as glutathione reductase (GR) and zinc homeostasis such as Zinc Transporter 1 (ZnT1). Speciation calculations showed variation of metal species depending on anionic media composition. Silver and cadmium showed affinity for chloride, copper for phosphate, and zinc remained primarily in its free ionic form. All metals complexed with cysteine avidly reducing metal toxicity, bioavailability and bioreactivity. Silver and copper toxicity were not affected by extracellular metal speciation, whereas cadmium and zinc toxicity were reduced by chloride complexation. Moreover, reduction of calcium in the medium increased toxicity and bioreactivity of cadmium and zinc. The bioavailability of non-essential metals was affected by media composition, while essential metals were tightly controlled by the cell in most media. For silver, low chloride reduced bioavailability while for cadmium bioavailability was increased by the presence of bicarbonate in the media. Non-essential metals induced increased GR and MT mRNA levels, zinc induced MT in all media excluding the control and cysteine media and copper induced MT only in the low chloride medium. ZnT1 was induced by cadmium in low-chloride media, by zinc in low-chloride low-calcium and by cadmium and copper in the no phosphate bicarbonate media. Overall, this study demonstrates that speciation alone is not sufficient to explain metal toxicity, and that many factors play a role in metal-cell interactions.

TABLE OF CONTENTS

LIST OF TABLES

Table Page

LIST OF FIGURES

Figure Page

INTRODUCTION

Chemical speciation is defined by International Union of Pure and Applied Chemistry (IUPAC) as: “specific form of an element defined as to isotopic composition, electronic or oxidation state, and/or complex or molecular structure” (McNaught et al., 1997). Metal speciation has been associated with aquatic metal toxicity for decades (Allen et al., 1980). Indeed, the link between environmental metal speciation and metal toxicity has been studied in a number of publications that demonstrated that free metal ions are the driving factor for metal uptake and metal toxicity, at least in fresh water (Campbell and Stokes, 1985; Niyogi and Wood, 2004). This research has led to metal bioavailability models (i.e. the Biotic Ligand Model and Free Ion Activity Model) that are reliable and beneficial to predict the toxicity of metals in aquatic organisms (Paquin et al., 2002; Pont et al., 2017). Thus, it is generally accepted that free metal ions compete at the biotic ligand, usually at the gill, wherein ions compete for entry depending on their affinity for the binding site in metal transporter proteins. This process can result in essential metal uptake as well as in non-essential metals hijacking essential metals or ions transport thus disrupting cellular homeostasis (Niyogi and Wood, 2004; Smith et al., 2015). Silver, for example, outcompetes sodium (Na) uptake at the gill, leading to a

decline in Na^+ and Cl^- uptake and rapidly ceasing carbonic anhydrase and Na^+/K^+-ATPase activity (Morgan et al., 2004). Moreover, several studies have shown that calcium has a protective function against divalent metals, such as iron (Fe) at the Divalent Metal Transporter 1 (DMT1), and cadmium (Cd), zinc (Zn) and copper (Cu) at calcium (Ca) channels (Franklin et al., 2005; Martinez-Finley et al., 2012; Walker et al., 2008).

In fresh water, the parameter that best predicts metal toxicity is chemical speciation (Reiley, 2007). In freshwater, fish do not drink, and the gill is the main route of uptake. However, in brackish and seawater fish drink for osmoregulatory purposes and the intestine becomes an important route of environmental metal exposure (Scott et al., 2006). The intestinal lumen environment possesses a wide assortment of both inorganic and organic ligands which readily bind metals forming metal complexes (Shehadeh and Gordon, 1969). Moreover, there is emerging evidence that metal complexes can be bioavailable and toxic at the intestinal epithelium (Ibrahim et al., 2020). This is supported by the fact that exposure to Cu, silver (Ag) or Cd across a salinity gradient, shows a decrease in metal toxicity from fresh water to brackish water but increases from brackish to seawater, demonstrating that metal toxicity across salinity is not linear (Grosell et al., 2007; Matson et al., 2016; Wang et al., 2016). These results suggest that as a fish transition from fresh to salt water, the increase in drinking rate leads to an increase in metal complexes in the gut lumen. This coincides with an increase in toxicity which suggests that the intestine might be the main route of exposure to metals in brackish water and saltwater fish and that metal complexes can be bioavailable and toxic.

The dynamic environment of the intestine causes variation in metal speciation depending on intestinal luminal composition (i.e. the composition of the intestinal juice) and can result in fluctuation in metal uptake and bioavailability (Bucking and Wood, 2006; Ojo and Wood, 2007, 2008). Indeed, the lumen of the gut has a great variety of organic ligands which has been shown to facilitate transport of essential metals such as Zn-gluconate and aminoacidic bound Zn, Cu and Mn (Antony Jesu Prabhu et al., 2018; Apines-Amar et al., 2004; Maage et al., 2001). Inorganic components have also been shown to influence uptake in human Caco2 cells, wherein Cu can be transported using an anion exchange transporter that requires chloride (Zimnicka et al., 2011). The role of Cl for Cu and silver uptake has also been shown to impact uptake in fish (Handy et al., 2000; Ibrahim et al., 2020). Although intestinal metal uptake is important in brackish and seawater the bioavailability and toxicity of metal complexes is poorly understood. This is partly due to the lack of an appropriate model to study these mechanisms and the complexity of the environment of the intestinal lumen.

Controlling the luminal composition of the intestine has been attempted before using the *ex vivo* gut sac model, in which the intestines are removed, the intestinal content is flushed away with physiological solution and then the intestines are prepped for exposure with synthetic exposure solutions (Grosell et al., 2005). However, this model possesses a short viability (4 hours), requires the harvesting of a fish for each replicate, and is reliant on the expertise of the handler (Handy et al., 2000). A valid alternative is the *in vitro* model of the fish intestine based on the rainbow trout (*Oncorhynchus mykiss*) gut cell line RTgutGC (Minghetti et al., 2017). RTgutGC cells

can adhere to the bottom of plastic multiwell plate and allow a tight control of the exposure medium which would not be possible *in vivo*.

Furthermore, the gut is the main route of uptake for the essential metal Cu, Zn and Fe whereas uptake at the gill can only occur during dietary metal deficiency (Bury et al., 2003; Kamunde et al., 2002). It has been calculated that uptake rates of the metals at the gut are similar to that of the gill, but the gut can achieve these uptake rates with a much smaller concentration of metal at the cellular surface (Ojo and Wood, 2007). Moreover, there is evidence that mechanisms of metal uptake at the gill and gut are different. For instance, Cu appears to be taken up at the intestinal epithelium using a transporter that is sodium independent (i.e. sodium and copper do not compete at the gut) whereas at the gill copper uptake can be affected by sodium concentration in the water (Handy et al., 2002). This suggests that at the gill Cu can leach thorough the sodium channel but at the intestine is transported by specific copper transporters, such as Copper Transporter 1 (CTR1) (Minghetti et al., 2008).

Essential metals are transported by specialized metal transporter proteins across the gut and gill epithelium. These transporters are characterized in families based on their metal specificity, such as zinc transporters (ZIP and ZnT), copper transporters (CTR), divalent metal transporters (DMT), etc. (Thevenod et al., 2019). In response to overburden of essential metals in the cell, pathways are initiated to use specialized excretory transporters, such as zinc transporters (ZnT), and Cu-ATPases (ATP7A and ATP7B) to relieve metal burden (Bury et al., 2003). Intracellular metal detoxification is controlled mainly by metallothionein (MT) a cysteine rich protein that is regulated by the Metal Transcription Factor (MTF-1) (Andrews, 2001). MTF1 can be considered a metal

sensor that regulates several genes involved in metal detoxification such as MT, and metal excretions such as ZnT1 and ATP7A/B (Gunther et al., 2012).

Molecular biomarkers are important as they can differentiate between inert and active bioaccumulated metals. For instance, it was shown that fish intestinal cells loaded with an identical concertation of dissolved silver (i.e. silver nitrate) or silver nanoparticles express higher levels of MT when exposed to dissolved silver (Minghetti et al., 2019). Glutathione reductase (GR) gene expression is induced in cells in response to oxidative stress (van der Oost et al., 2003). Furthermore, increase of GR mRNA levels in response to metal burden in fish has been shown previously (Minghetti et al., 2008; Minghetti and Schirmer, 2016). Metallothionine is a known biomarker for both non-essential and essential metal exposure (Coyle et al., 2002). ZnT1 is used for efflux of Zn out of the cell and can be utilized by the cell to reduce intracellular zinc burden (Zheng et al., 2008). An increase in these genes represents a cellular response to metal overburden, which allows to determine the relationship between metal accumulation and metal bioreactivity.

Therefore, in this study I have set out to determine the relationship between metal complexation and competition in the exposure medium with metal bioavailability, toxicity and bioreactivity in RTgutGC cells. Metal speciation was manipulated by designing specific synthetic media. These media were used to dissolve two essential (Cu and Zn) and two non-essential (Ag and Cd) metals. To quantify the effects of different metal species, I measured their bioavailability, toxicity and bioreactivity in RTgutGC cells. Comparing these cellular effects, this study will show the link between intestinal lumen composition and metal bioavailability and toxicity, ultimately implementing our understanding of metal uptake processes at the cell-intestinal lumen interface.

METHODS

Media Preparation and Speciation Calculations

Metal speciation and precipitation calculations were performed using the software Visual MINTEQ version 3.1 (Gustafsson, 2013). All the media designed for this experiment are derived from the commercial medium Leibovitz's L-15 which is used to culture RTgutGC cells. However, all amino acids and vitamins were removed from L-15 to inhibit metal complexations. The exposure medium is thus called L-15/ex. Moreover, five medium components, which affect metal speciation, were altered in L-15/ex (i.e. Ca^{+2}, Cl^{-}, PO_4^{-3}, CO_3^{-2} and cysteine (Cys); Table 1). To maintain pH, osmolality, and ionic strength, other components were added to the media (i.e. NO_3^{-}, and HEPES; Table 1).

Chloride was chosen due to its abundance in salt water and brackish water environment, its role in metal uptake and its high affinity for Ag and Cd. While phosphate (PO_4) and bicarbonate (HCO_3) were chosen for their role in intestinal physiology and affinity for divalent metals (Grosell et al., 2005; Kurita et al., 2008). Calcium was chosen due to its ability to compete with the divalent metals (Cd^{2+}, Cu^{2+} and Zn^{2+}) (Niyogi and Wood, 2004). Lastly, cysteine was chosen due to its known role in

metal detoxification (Minghetti and Schirmer, 2016). L-15/ex contains high chloride concentration which can result in metal complexation (Ibrahim et al., 2020). Therefore, to reduce the concentration of chloride complexes two media were prepared with low Cl, (L-15/Cl_{Low}) and low Cl and low calcium (L-15/Cl_{Low}-Ca_{Low}). Both media contain 1 mM Cl, while L-15/Cl_{Low}-Ca_{Low} also has Ca lowered to 0.075 mM. Moreover, the role of phosphate complexation was tested by removing it from the medium. Two media were PO_4^{-3} free, L-15/P_{Free} and L-15/HCO_3^-. In L-15/P_{Free}, phosphate was substituted with HEPES and 5 mM HCO_3^- was added to L-15/P_{Free} to create L-15/HCO_3^-. L-15/Cys consisted of L-15/ex with 0.5 mM L-Cysteine added, just prior to exposure. The 0.5 mM concentration of cysteine was chosen as it was far greater than any dose used, allowing for maximum chelation of metals.

Speciation calculation within each media was done by incremental addition and subtraction of the compounds in Visual Minteq to obtain the desired metal species profile. Negligible changes were observed in each specific medium in metal speciation at concentration ranging from 0.1 to 500 µM. Due to this, metal speciation calculations in each media, 200 µM of Ag, Cd, Cu, and Zn were used. Calculated values by Visual Minteq are presented as percentages of total metal in the media. A complete list of media and media composition can be found in Table 1. Metal complexes precipitation was calculated by adjusting the metal concentration in each media.

Osmolality and pH of each media were measured using the Vapro® Vapor Pressure Osmometer (Model5600, ELItech group, South Logan, UT, USA) and SI Analytics pH meter (SI Analytics, College Station, TX, USA), respectively.

RTgutGC Cell Culture

RTgutGC cells were cultured in 75 cm^2 cell culture flasks (Greiner Bio One, Monroe, NC, USA) in the complete medium (L-15/FBS) at 19 ºC in a normal atmosphere incubator. L-15/FBS is Leibovitz L-15 medium (Thermo Scientific, Waltham, MA, USA) supplemented with 5 % Fetal Bovine Serum (FBS, Sigma-Aldrich, St. Louis, MO, USA) and gentamicin (10 mg/L; Sigma-Aldrich, St. Louis, MO, USA). Once the cells reached approximately 90% confluence, they were washed twice with versene solution (Thermo Scientific, Waltham, MA, USA) and detached from the flask using 0.25% trypsin (Thermo Scientific, Waltham, MA, USA). Cells were resuspended in L-15/FBS and the cell concentration was measured using a Countess II^{TM} Automated Cell Counter (Life Technologies Corporation, NYC, NY, USA) using a sample of the cell suspension. Cells were diluted with L-15/FBS to allow for a seeding density of 73,684 cells per cm^2 per well on a Greiner 6- or 24-well plate (Greiner Bio-One, Monroe, NC, USA). This density was achieved by seeding 140,000 cells in 24 well plates. Each well has surface area of 1.9 cm^2. Cells were then incubated at 19 ºC for 48 hours to allow the formation of a confluent cell monolayer.

Exposure

For exposure we mean the application of the experimental media (Table 1) containing metals on RTgutGC monolayers. Six concentrations of each metal in each media were used for each exposure to create a dose response curve. Silver concentrations were set to 50, 10, 2, 1, 0.4, and 0.08 µM, Cadmium's and Cu's concentrations were 200, 40, 20, 5, 0.5, and 0.1 µM, and Zn's concentrations were 500, 100, 50, 25, 5, and 1 µM

(Table 4). All exposure solutions were made just before cell exposure to minimize the effects of precipitation and allow for an accurate exposure concentration.

To test the role of cysteine complexation on metal toxicity in RTgutGC cells were prepared as stated above and exposed to metals in L-15/ex and L-15/Cys (Table 1). Metals were spiked as described above into both L-15/ex and L-15/Cys at concentrations near their individual EC_{50} (Ag: 1 µM, Cd: 20 µM, Cu: 5 µM, and Zn:100 µM). Cells were exposed to the mixtures (in quadruplicate) and incubated at 19ºC for 24 hours. After exposure the cytotoxicity assay was performed as described above.

Stock solutions of $AgNO_3$, CuSO4.5H2O, $ZnSO_4.7H_2O$, and $CdCl_2$ (Sigma-Aldrich, St. Louis, MO, USA) were prepared at 10 mM concentration in ultrapure water (16–18 mΩ, Barnstead GenPure Water, Thermo Fisher Scientific, Waltham, MA, USA). Exposure solutions were freshly prepared by spiking the a concentrated metal solution in ultrapure water in the respective exposure media at metal concentrations ranging from 0.08 and 500 µM (Table 4), vortexed for 20 s and immediately added to the washed cell monolayers. Spike volumes were no larger than 5% the final exposure stock volume to minimize dilution of media components. Stock solutions and exposure solutions with a nominal solution of 10 µM were measured by ICP-OES, and nominal concentrations were confirmed to be within 10% of measured concentrations (Table 5). All reported concentrations are nominal.

Before exposure, cells were washed twice with their respective media to remove all traces of L-15/FBS from the well. Afterwards metal solutions at different

concentrations were applied onto the cell monolayers, in triplicate, and cells were incubated at 19 ºC for 24 hours before viability was measured.

Cytotoxicity

Cytotoxicity is defined as the overall effect of metal exposure on cell viability and the first step in determining the toxicity of metal species to the cell (Morcillo et al., 2016). Cell viability was measured using a three-endpoint cytotoxicity assay using 3 fluorescent dyes. Alamar Blue (Resazurin; Invitrogen, Eugene, OR, USA), CFDA-AM (5-carboxyfluorescein diacetate acetoxymethyl ester; Invitrogen, Eugene, OR, USA), and Neutral Red (3-Amino-7-dimethylamino-2-methylphenazine hydrochloride; Invitrogen, Eugene, OR, USA), in accordance with the methods of Schirmer et al. (1997). Alamar Blue, CFDA-AM, and Neutral Red can be used as cellular markers of metabolic activity, cell membrane integrity and lysosome integrity (Minghetti and Schirmer 2016). Alamar Blue, CFDA-AM and Neutral Red excitation/emission were read via the Cytation 5 plate reader at 530/595, 485/530 and 530/645 nm wavelength, respectively. Dose response curves for each condition tested are reported as % viability based on the blank corrected (i.e. fluorescence of the dyes applied on an empty cell free well) fluorescence units (FU) of the untreated cells (i.e. L-15/ex control) and can be found using the following equation:

$$\%\ of\ control = \frac{FU_{exposed\ cells} - FU_{blank}}{Average[FU_{control\ cells} - FU_{blank}]} \times 100$$

Bioavailability

Bioavailability is defined as the total metal concentration measured in the cell. Cells were seeded at a density of 73,684 cells*cm^{-2} as previously described but in 6-well

plates (Greiner Bio-One, Monroe, NC, USA). After incubation and washing cells were exposed to 600 nM of each metal in an identical fashion to the cytotoxicity assay. Cells were exposed for 24 hours and incubated at 19ºC. After exposure, a 1 mL sample of each exposure media was collected and acidified with 5% nitric acid for ICP-OES measurement. After a 24-hour exposure, each well was washed twice with 1 mL of 0.5 mM cysteine dissolved in PBS to remove any loosely bound extracellular metal. After washing, cells were lysed using 1 mL of 50 mM NaOH solution and the plates were incubated at room temperature and mixed at 200 rpm for 2 hours using an orbital shaker (VWR Advanced Mini Shaker 15). After mixing, the cell lysates were carefully transferred into 1.7 mL Eppendorf tubes and a 100 µL aliquot was taken for total protein quantification using the modified Lowry assay (Thermo Scientific, Waltham, MA, USA). The remaining 900 µL were desiccated using a concentrator (concentrator plus, Eppendorf, Hauppauge, USA). Desiccated samples were then digested for 16 hours using 0.8 mL of 68% HNO_3 at room temperature to allow for complete dissolution of all the metals. Sample digestion was finalized by adding 0.2 mL of H_2O_2 and incubated at room temperature for one hour. The whole solution was transferred to a 15 mL falcon tube and diluted to a final nitric acid concentration of 5%. Samples were stored at 4ºC until the ICP-MS (iCAP Qc, Thermo Fisher Scientific, Driesch, Germany) analysis. Standard reference material (NIST SRM 1643f; National Institute of Standards and Technology, MD, USA) was analyzed with each set of samples for quality control. To control for the variation in total cell numbers per well, all metal concentrations are normalized by protein content and reported in ng of metal/mg of protein.

Bio-reactivity

In this study, bio-reactivity is defined as the measurement of specific metal-responsive gene (i.e. MT, GR and ZnT1) mRNA levels in RTgutGC cells. For the bio-reactivity assay, cells were seeded at a density of 73,684 cells*cm^{-2} in 6-well plates (Greiner Bio-One, Monroe, NC, USA) and exposed to 600 nM of each metal in an identical fashion to the bioavailability experiment and incubated at 19°C for 24 hours. After exposure, cells were washed once with each respective media, to remove excess metal. The wash solution was removed, and 900 µL TriZol reagent (Thermo Fisher Scientific, Waltham, MA, USA) was added to lyse the cells. RNA was extracted following the manufacturer instructions. The purified RNA was treated with the TURBO DNase kit (Thermo Fisher Scientific, Waltham, MA, USA) to remove any trace of DNA. Quality and quantity of RNA was determined spectrophotometrically using Cytation 5 Plate Reader (Bio-Tek, Winooski, VT, USA) and by electrophoresis using 1 µg of RNA in 1% agarose gel. Complementary DNA (cDNA) synthesis was performed from 1 µg of total RNA using Maxima H Minus First Strand cDNA synthesis Kit (Thermo Fisher Scientific, Waltham, MA, USA) by following manufacturer instructions. Quantitative PCR (qPCR) was performed in triplicate using the SYBR premix Ex Taq II (Clontech, Mountain View, CA, USA) for MT and the CFX Connect Real-Time PCR Detection System (BioRad, Hercules, CA, USA) for all other genes. Messenger RNA (mRNA) levels were measured using the absolute quantification method and are reported as fold change of the treated groups from control. Metallothionein (MT), Glutathione reductase (GR) and zinc transporter 1 (ZnT1) were measured for bio-reactivity. Normalization of copy number of the target genes was performed using the geometric means of the

reference genes (Elongation factor 1a and Ubiquitin). All conditions were normalized between plates using 4 internal control (IC) samples. IC were cells exposed to the complete medium L-15/FBS. The plate selected for IC normalization was determined by the PCR efficiency closest to 100%. Primer sequences are reported in Table 6. The qPCR efficiency for all genes was above 90%. Detailed procedures on RNA extraction, DNase treatment, cDNA synthesis, and qPCR measurement of mRNA levels of target genes have been described previously in Minghetti et al. (2014).

Statistics

Statistical analysis was performed using GraphPad Prism Version 8 (GraphPad Software Inc., San Diego, CA). The effective concentration 50 (EC_{50}) was calculated by nonlinear regression sigmoidal dose-response curve fitting module using the Hill-slope equation (Gadagkar and Call, 2015). EC_{50}s are presented as the mean plus or minus the standard deviation ($n \geq 3$). The geometric mean (geomean) of all three viability endpoints was used when comparing cytotoxicity among the metals and during correlation statistics of cytotoxicity and speciation. Correlations between the percentage of total metal of a specific metal species and the EC_{50} value were analyzed using the Pearson's R correlation coefficient ($p < 0.05$). Analysis of variance (ANOVA) followed by Tukey's post hoc test was performed to determine the statistical significance among the different experimental groups. Dunnett's post hoc test was substituted for Tukey's when comparing test samples to control ($p < 0.05$). All data were assessed for normality and homogeneity using the D'Agostino & Pearson normality test and the Brown-Forsythe test, respectively (Mbah and Paothong, 2014; Parra-Frutos, 2012). Where necessary, sample data were logarithm base 10 transformed to improve normality.

RESULTS

Speciation

Metal speciation and precipitation results are reported in Figure 1 and dominant species in Table 2. The reduction of chloride concentration in L-15/Cl_{Low} and L-15/Cl_{Low}-Ca_{Low} media and addition of L-cysteine in L-15/Cys affected both Ag and Cd speciation. A change to any component other than chloride and cysteine did not change speciation of these metals in comparison to the control medium L-15/ex. Ag and Cd speciation was dominated by neutral and negatively charged $MeCl_n$ species at high Cl concentrations in L-15/ex but at the low chloride levels the concentration of the free Me ion ($Me^{+1/2}$) become the dominant species. Copper speciation was affected by varying the concentration of PO_4^{+2}, HCO_3^{-1}, and cysteine, wherein $CuCO_3$ and CuCys were dominant in L-15/HCO_3^- and L-15/Cys, respectively. In L-15/ex, L-15/Cl_{Low}, and L-15/Cl_{Low}-Ca_{Low}, Cu's dominant species was the free ionic species Cu^{2+} and $CuHPO_4$ was the second most abundant species. Similarly, in the phosphate free medium, the free ionic species was the most dominant species, while the second largest species were hydroxide Cu species, $Cu_3(OH)_4^{+2}$, and $Cu_2(OH)_2^{+2}$ accounting for a combined 49.95% of Cu present. The introduction of carbonate produces the species $CuCO_3$ surpassing the free copper ion with a calculated 63.0% in L-15/HCO_3^-. Zn speciation was affected by the presence of

cysteine in the medium, where Zn_nCys_n was dominant. In the other media, Zinc speciation is dominated by the free ion species, ranging from 75% to 85% of the total dissolved metal. Minor zinc speciation changes occurred in the non-dominant species in the low Cl media (Cl_{Low} and Cl_{Low}-Ca_{Low}) and in the phosphorous free media where $ZnHPO_{4(aq)}$ and $ZnCl^+$ where the second most abundant species. All metals showed a very high affinity for cysteine which resulted in metal-cysteine complexation of over 90% of the total metal species in the media.

Speciation did not change significantly with metal concentration in solution, whereas precipitation was strongly related to metal concentration as well as the media composition. All precipitation values can be found in Table 3, while 1% and 50% precipitation are denoted on Figure 1. Ag precipitated in all of the media as cerargyrite ($AgCl_{(s)}$). Silver precipitation started (i.e. at 1% metal concentration) at 4.65, 0.4, 0.45, 0.37, and 0.37 µM for L-15/ex, L-15/Cl_{Low}, L-15/Cl_{Low}-Ca_{Low}, L-15/P_{FREE} and L-15/HCO_3^-, respectively. Cadmium did not precipitate in the media containing high Cl concentration (168 mM) but at low Cl concentration (1 mM; L-15/Cl_{Low} and L-15/Cl_{Low}-Ca_{Low}) Cd started to precipitate as $Cd_3(PO_4)_2$ when added above 67.5 µM. Copper precipitation started (1% of total metal) at 3.13, 3.86, 3.1, 1.77, 1.18, and 3.13 µM in, L-15/ex, L-15/Cl_{Low}, L-15/Cl_{Low}-Ca_{Low}, L-15/P_{Free}, L-15/ HCO_3^- and L-15/Cys. respectively. The precipitate was $Cu_3(PO_4)_2$ in L-15/ex, L-15/Cl_{Low} and L-15/Cl_{Low}-Ca_{Low}, brochantite (Cu4SO4(OH)6) in L-15/P_{Free} and as azurite ($Cu_3(CO_3)_2(OH)_2$) in L-15/ HCO_3^-. Zinc did not precipitate up to 500 µM in L-15/P_{FREE} and 200 µM L-15/Cys, while it precipitated (1% of total metal) in L-15/ex, L-15/Cl_{Low}, and L-15/Cl_{Low}-Ca_{Low} as $Zn_3(PO_4)_2$:$4H_2O$ at

5.7, 6, and 6.2 µM, respectively, and in L-15/HCO_3^- at 14.3 µM as hydrozincite ($Zn_5(CO_3)_2(OH)_6$).

Cytotoxicity

Cytotoxicity results are shown in Figure 2 and EC_{50} values are reported also in Table 6. The cytotoxicity dose-response curves are pictured in Figure 3. The geomean EC_{50} hierarchy was Ag>Cu>Cd>Zn for metals dissolved in L-15/ex ($P< 0.001$), Ag = Cu > Cd > Zn for L-15/Cl_{Low} and L-15/HCO_3^- ($p<0.05$), Ag > Cu > Cd = Zn for L-15/ Cl_{Low}-Ca_{Low} ($p < 0.001$) and Ag = Cu = Cd ≥ Zn (where Ag > Zn and Cu > Zn) for L-15/P_{Free} ($p = 0.013$).

Silver toxicity was not affected by the media composition in RTgutGC cells, except for L-15/HCO_3^- where silver was less toxic in comparison to the low chloride medium in metabolic activity only ($p = 0.017$). Similarly, Cu was not affected by the media composition for two of the three endpoints ($p > 0.05$). Lysosome integrity was affected significantly less by copper in L-15/ex in comparison to all other media ($p < 0.001$).

Conversely, cadmium toxicity was affected by the media composition. Cadmium was between 10- and 17-fold more toxic to cells, depending on the endpoint measured, in the low chloride, low calcium medium (Cl_{Low}-Ca_{Low}) than in in the reference medium L-15/ex ($p < 0.001$). Similarly, cells exposed to cadmium in L-15/P_{Free} media showed a 3.5-fold reduction in metabolic activity than cells in L-15/ex ($p = 0.019$). Cells exposed in L-15/HCO_3^- showed a 7.1- and 3.7-fold reduction in metabolic activity ($p < 0.001$), and lysosome integrity ($p = 0.003$), respectively, compared to cells exposed in L-15/ex.

Similarly, Zn toxicity was increased by the reduction in chloride, calcium and phosphate in the medium. Moreover, toxicity was increased further by the addition of bicarbonate to the exposure medium. Cellular metabolic activity was reduced by Zn in all of the manipulated media compared to L-15/ex, with L-15/Cl_{Low}-Ca_{Low} ($p < 0.001$) and L-15/HCO_3^- ($p < 0.001$) being the most toxic at 5.7- and 7.1-fold more toxic than L-15/ex, respectively. Membrane integrity was reduced by Zn in L-15/Cl_{Low}-Ca_{Low} of 5.1-fold in comparison to L-15/ex ($p = 0.030$). Lysosome integrity in cells exposed in L-15/HCO_3^- was reduced 3.7-fold in comparison to cells exposed in L-15/ex ($p < 0.014$).

The introduction of cysteine in the exposure medium reduced the toxicity of all metals in at least two of the three endpoints ($p < 0.05$; Figure 5). Metabolic activity was significantly protected by cysteine in the cells exposed to all four metals ($p < 0.05$). Membrane integrity was only protected by cysteine in Zn exposures. Lysosome integrity was protected against Ag ($p = 0.002$), Cd ($p = 0.036$), and Cu ($p = 0.041$; Figure 5).

Geomean EC_{50} values did not correlate with any of the metal species forming in the exposure media ($p > 0.05$; Figure 4). Three species for each metal were tested for correlation. Silver was the metal that trended the most towards a species-toxicity correlation but was still not significant: Ag^+ ($p = 0.327$), $AgCl_{(aq)}$ ($p = 0.349$), and $AgCl_2^-{}_{(aq)}$ ($p = 0.310$). The Cd species correlations were: Cd^{2+} ($p = 0.776$), $CdCl^+$ ($p = 0.676$), and $CdCl_{2\,(aq)}$ ($p = 0.840$). The three species of Cu were: Cu^{2+} ($p = 0.264$), $CuCl^+$, ($p = 0.855$), and $CuSO_{4\,(aq)}$ ($p = 0.380$). The species of Zn correlated were: Zn^{2+} ($p = 0.543$), $ZnCl^+$ ($p = 0.971$), and $ZnSO_{4\,(aq)}$ ($p = 0.714$).

Bioavailability

Metal bioavailability in RTgutGC is reported in Figure 6. Silver was less (3.3- to 7.0-fold) bioavailable in L-15/Cl_{Low}, and L-15/Cys in comparison to L-15/ HCO_3^- and L-15/ex, ($p < 0.05$). Cells exposed to Ag in low Cl media (L-15/Cl_{Low} and L-15/Cl_{Low}-Ca_{Low}) showed noticeable stress to the exposure (i.e. vacuolization and cell detachment; Figure 10). This was not observed in any other condition. Copper was 2.3-fold more bioavailable in L-15/Cl_{Low} compared to the reference media (L-15/ex) and was significantly greater than all of the media ($p < 0.001$). Cadmium was more bioavailable in L-15/Cl_{Low} (2.0-Fold; $p < 0.001$), L-15/Cl_{Low}-Ca_{Low} (1.8-fold; $p = 0.002$) and L-15/HCO_3^- (2.5-fold $p < 0.001$) when compared to L-15/ex. In L-15/Cl_{Low}, Zn bioavailability was 3.6-fold less, on average, then all of the other media in the cells ($p < 0.05$). Zinc bioavailability was higher in L-15/Cl_{Low}-Ca_{Low} than in L-15/HCO_3^- (1.4-fold; $p = 0.027$) and in L-15/Cys (1.5-fold; $p = 0.011$; Figure 6).

Bio-reactivity

The mRNA levels of GR, MT and ZnT1 were measured in cells exposed to metals and can be found in Table 8. Messenger RNA copy numbers for each test condition, including control unexposed cells, are reported in Figure 8. The effect of the media alone, (i.e. without metal) was evaluated. Cells exposed to L-15/Cl_{Low} and L-15/HCO_3^- showed a reduction in GR expression of 1.8- and 2.5-fold in mean expression in comparison to the levels found in cells exposed to L-15/ex ($p < 0.05$). The cells in L-15/Cl_{Low}-Ca_{Low} showed higher levels (2.1- to 10.8-fold; $p < 0.05$) of MT mRNA in comparison to the levels measure in cells in all other media. Cells cultured in L-15/Cys showed the lowest MT mRNA levels than cells cultured in all other exposure conditions (3.1- to 10.8-fold; $p < 0.05$). Finally, cells exposed to L-15/Cl_{Low}-Ca_{Low} and L-15/HCO_3^- media expressed

significantly less ZnT1 than cells exposed in the L-15/ex at 2.2- and 4.0 the mean expression in L-15/ex ($p < 0.05$). ZnT1 was expressed at similar levels in all media.

Cells exposed to Ag in L-15/HCO_3^-, showed the largest induction in GR mRNA levels, 3-fold higher than control ($p < 0.001$). Moreover, GR mRNA levels were higher than control in cells exposed to Cd in L-15/Cl_{Low} (1.4-fold; $p = 0.012$) and in L-15/HCO_3^- (1.4-fold; $p = 0.004$). Zinc induced a significant increase in GR mRNA levels in cells exposed in Cl_{Low}-Ca_{Low} (1.5-fold; $p = 0.004$).

Cells exposed to Ag and Cd showed the largest MT fold change induction, ranging from 5 to 30 times higher than control, in all media excluding L-15/Cys were MT was induced only by Cd. The highest MT fold change induction was in cells exposed to Ag and Cd in L-15/HCO_3^-, at 28- and 27-fold, respectively ($p < 0.05$). Cells exposed to Zn showed a 3.8-, 9.4- and 4.5-fold increase in MT mRNA levels in L-15/Cl_{Low}, L-15/Cl_{Low}-Ca_{Low}, and L-15/HCO_3^-, respectively ($p < 0.05$). Metallothionein was not induced by Zn exposure in L-15/ex and L-15/Cys media ($p > 0.05$). Copper induced an increase in MT mRNA levels compared to controls only in Cl_{Low} and HCO_3^- media at 2.3- and 2.8-fold, respectively ($p < 0.05$).

ZnT1 mRNA levels were not affected by any of the metals in cells exposed in L-15/ex and L-15/Cys ($p< 0.05$). Cells exposed to Cd in low chloride medium (Cl_{Low}) and in bicarbonate (HCO_3^-) medium showed an increase of 2.7- and 2.6-fold compared to respective controls, respectively ($p < 0.05$). Zinc exposure in low chloride low calcium medium (Cl_{Low}-Ca_{Low}) increased ZnT1 mRNA levels by 2.8-fold ($p = 0.001$) in

comparison to respective controls while Cu exposure in the bicarbonate media (HCO_3^-) induced a 2.5-fold increase in ZnT1 mRNA levels ($p = 0.007$).

DISCUSSION

This study set out to show the relation between metal speciation in the exposure medium and metal toxicity, bioavailability and bioreactivity in the RTgutGC cell line. I used a novel combination of speciation modeling, cytotoxicity, ICP-MS, and qPCR to demonstrate a comprehensive *in vitro* approach to study the exposure conditions that could enhance or reduce metal toxicity at the fish intestinal epithelium. The toxicity hierarchy of the metals in L-15/ex was Ag > Cu > Cd > Zn confirming our previous results (Ibrahim et al., 2020). However, the metal toxicity hierarchies were modified by media manipulations: Ag = Cu > Cd > Zn for L-15/Cl_{Low}, Ag > Cu > Cd = Zn for L-15/Cl_{Low}-Ca_{Low}, Ag = Cu = Cd ≥ Zn for L-15/P_{Free} and Ag = Cu > Cd > Zn for L-15/HCO_3^-. However, these changes in toxicity cannot be correlated to any one species for any of the metals (Figure 4; Table 7). These results showed that metal speciation alone cannot explain the overall toxicity and bioavailability of metals in the epithelia of the fish gut further confirming our previous results (Ibrahim et al., 2020).

Cysteine is a sulfur containing amino acid used throughout the cell and it is an integral part of the MT and glutathione structures (Giles et al., 2003). Cysteine rich proteins, such as MT, can bind free metals in the cytoplasm with high affinity and

mitigate toxicity (Gunther et al., 2012; Minghetti and Schirmer, 2016). Indeed, the addition of 0.5 mM cysteine protected the cells from non-essential metal accumulation and reduced metal bio-reactivity and toxicity (Table 2; Table 5; Table 8). This supports the role of cysteine as a metal chelator and scavenger of metal toxicity and its key role in MT and the MTF-1 pathway (Gunther et al., 2012). The essential metals, Cu and Zn, bound to cysteine were as bioavailable as the free metal ions, Cu^{2+} and Zn^{2+}. Moreover, these results suggest that chelated Cu and Zn (CuCys and Zn_nCys_n) species are bioavailable, supporting previous evidence on the importance of aminoacidic chelation on essential metal transport (Antony Jesu Prabhu et al., 2018; Vercauteren and Blust, 1996).

In the sections below, I will discuss the specific media interactions and cellular effects which are unique for each metal in RTgutGC cells.

Silver

Several studies have shown that chloride concentration in the exposure medium can affect metal bioavailability. Chloride is a key compound for water balance in the gut, as well as a vital anion in both symporters and antiporters (Grosell and Taylor, 2007). In addition, several studies have shown that Cl has a protective effect against Ag toxicity and accumulation especially in freshwater fish where metal uptake occurs mainly at the gill (Bielmyer et al., 2008; Niyogi and Wood, 2004; Wood et al., 2002). However, even with silver speciation shifting from $AgCl_n$ negatively charged species in the high chloride media (L-15/ex, L-15/P_{Free}, L-15/HCO_3^-) to the free silver ion in low chloride media (L-15/Cl_{Low}, L-15/Cl_{Low}-Ca_{Low}; Figure 1), I did not measure any statistical difference in toxicity between the two Ag species. This is inconsistent with fresh water models which

suggest that free metals exert the most toxicity on the cells (Niyogi and Wood, 2004). However, in RTgutGC cells, Ag accumulated 7 times less in L-15/Cl_{Low}, compared to the reference media (L-15/ex; Figure 2) suggesting the free ion is more toxic but not as bioavailable thus resulting in equal toxicity. This is further confirmed by observations made during the bioavailability experiment where cells exposed in the low Cl media showed vacuolization and cell detachment which are indicators of cell stress (Figure 10).

In the low Cl low Ca medium, silver bioavailability, bio-reactivity and toxicity were similar to that in L-15/ex, suggesting Ca does play a protective role in silver uptake. This supports the hypothesis that in the gut, Ag uptake likely occurs via CTR1, a calcium independent transporter, whereas at the gill it mostly occurs via the Na^+ channels (Burke and Handy, 2005; Minghetti and Schirmer, 2016).

Cells exposed to silver in L-15/HCO_3^- had similar bioavailability to L-15/Ex, with $AgCl_{(aq)}$ as the dominate species in both media. However, cells exposed to Ag in L-15/HCO_3^- showed the largest increase in MT expression (30-fold). This suggests that Ag in the presence of bicarbonate is more bio-reactive and toxic without speciation change. The role of HCO_3^- is still unclear in metal toxicity, however, it has been shown that the basolateral side of the cell does have a HCO_3^-/Na^+ antiporter which could facilitate movement of Ag^+ out of the cell (Kurita et al., 2008). In this study, RTgutGC were seeded on regular wells, thus were not polarized cells which could allow for these transporters to be expressed on the apical side of the cell. Future studies into this effect should use polarized cells to elucidate this effect.

Cadmium

Cadmium toxicity was significantly affected by media composition. Indeed, cells exposed to Cd in low chloride, low calcium medium (L-15/Cl_{Low}-Ca_{Low}), where Cd^{2+} was the dominant species, showed toxicity between 4.65 and 20 times higher than cells exposed to Cd in high chloride, high calcium medium (L-15/ex) where chloride complexation dominated (Figure 2; Figure 6). This supports the FIAM and BLM assumptions suggesting that the free Cd^{2+} is the most toxic species for intestinal cells and that calcium has a protective role against cadmium toxicity (Niyogi and Wood, 2004; Ojo and Wood, 2008). Indeed, Ca has long been associated with metal toxicity. Its protective role was previously shown as metal toxicity is inversely correlated with water hardness (Paquin et al., 2002). Past research supports the concept that competition at the cell's membrane between divalent metals can inhibit divalent metal toxicity (Franklin et al., 2005; McRae et al., 2016; Walker et al., 2008), with the two major locations of competition being DMT1 and Ca Channels, where Cd has been shown to enter the cell (Ojo and Wood, 2008).

Cadmium bioavailability and bio-reactivity was also highly dependent on chloride complexation and supports previous studies where Cd^{2+} was shown to be the most toxic and bioavailable species in eukaryotic cells (Thevenod et al., 2019). Upon entering the cell through divalent metal transporters (e.g. Ca channels, ZiP, DMT1 transporters), Cd binds MT readily, displacing Zn, initiating the MTF-1 pathway (Hardyman et al., 2016). This in turn upregulates ZnT1, to export metal excess. However, ZnT1 preferentially binds to Zn^{2+} over Cd^{2+} leading to inefficient excretion of Cd and Cd bioaccumulation

(Hoch et al., 2012). Our data supports these studies and demonstrates the efficacy of the RTgutGC model.

Bicarbonate's role on water balance, ionoregulation and pH balance within the cell demonstrates its importance but it was also shown to be important with regards to metal uptake and toxicity (Grosell et al., 2005; Nebert et al., 2012). The protective effect by chloride complexation with Cd was inhibited by HCO_3^- which increased cadmium toxicity bioavailability and bioreactivity to the levels shown in cells exposed in low chloride low calcium medium (Figure 2; Figure 6; Figure 7). The role of HCO_3^- on Cd bioavailability and toxicity has not been extensively investigated, however, HCO_3^- has been shown to facilitate Cd transport into the cell through a $Zn^{2+}/[HCO_3^-]_2$ symporter (Liu et al., 2008), leading to higher bioavailability of Cd in the cell. The fact that L-15/HCO_3^- elicited similar bioaccumulation, cytotoxicity, and GR and ZnT1 gene expression to L-15/Cl_{Low}-Ca_{Low} but MT was 5.2-fold higher in L-15/HCO_3^-, suggests that intracellular Cd processing might be different and result in higher Cd bio-reactivity. The elucidation of this mechanism will require further studies.

Copper

The increased bioavailability in low chloride medium (L-15/Cl_{Low}) is not easy to explain (Figure 6). Previous studies in mammalian intestinal cells (Zimnicka et al., 2011) and in fish *ex vivo* models (Handy et al., 2000) showed that copper uptake decreases with a corresponding decrease in luminal chloride concentrations. This may be due to their use of polarized Caco2 cells (human) on transwells and media with no Cl^- present while this study used RTgutGC (rainbow trout) in standard wells with 1 mM Cl concentration (Table 1).

Copper in the HCO_3^- medium resulted in an increase of ZnT1 expression compared to control and other media with Cu (Table 6;

Table 7). The cell can use bicarbonate, a waste anion, in an antiport fashion moving nutrient ions from the lumen to the cytoplasm and then to the plasma (Ando and Subramanyam, 1990; Kurita et al., 2008). This movement of bicarbonate can be utilized by the cell for transport of essential nutrients such as Cl^-, and Zn^{2+}, as well as Cd^{2+} (Nebert et al., 2012).These results are congruent with the research, as Cu has been shown to have anionic dependent uptake pathways, such as Cl^- and HCO_3^- (Handy et al., 2000; Zimnicka et al., 2011). Overall, the relationship between Cu and HCO_3^- is still not fully understood. However, these data do suggest that HCO_3^- has some influence on Cu toxicity, possibly increasing coppers bioavailability.

Zinc

Excluding the addition of cysteine, Zn speciation was not affected by any of the other variation in media composition (Figure 1). Media composition however, affected the toxicity and bioavailability of zinc, with the most toxic media being L-15/Cl_{Low}-Ca_{Low} (Figure 2; Figure 5) thus showing an effect similar to cadmium toxicity. Past studies looking into the relationship of Zn^{2+} bioaccumulation and calcium concentration have shown that Zn can use DMT1 (Martinez-Finley et al., 2012; Niyogi and Wood, 2004). The L-15/Cl_{Low}-Ca_{Low} medium induced the highest zinc bio-reactivity as shown by MT and ZnT1 gene expression measurements (Figure 8). This effect is supported by past research into Zn toxicity in which the cells respond with higher levels of MT and ZnT1 for Zn toxicity remediation, both of which are regulated through the MTF1 pathway (Andrews, 2001; Gunther et al., 2012).

Similarly to Cu, Zn caused higher expression of MT and toxicity in RTgutGC cells in the L-15/HCO_3^- medium. This result can be explained by the fact that Zn can use

$Zn^{2+}/[HCO_3^-]_2$ antiporter for intracellular influx of Zn into the cytosol leading to MT induction (Gunther et al., 2012; Liu et al., 2008).

Internal Zn concentrations significantly dropped in cells with L-15/Cl_{Low}, while MT expression increased 3.8-fold higher than control. This latter effect implies an increase in free cytoplasmic Zn^{2+} which could induce excessive zinc excretion through ZnT1 in L-15/Cl_{Low}. The reduction in Zn bioavailability was not shown with the reduction of Ca in L-15/Cl_{Low}-Ca_{Low} medium. This is expected, as Ca^{2+} competes with Zn^{2+} at Ca channels (McRae et al., 2016) which would result in an increase in Zn bioavailability. Moreover, low Ca effects resulted in higher gene expression of both MT (9.4-fold) and ZnT1 (2.8-fold), as well as higher toxicity. These results show that even though low Cl may induce an overexcretion of Zn, the lack of Ca results in more uptake of Zn^{2+} requiring the cell to counteract the metal burden with higher metal homeostatic and chelating processes

CONCLUSION

This study shows the impact of medium components such as inorganic and organic anions on metal toxicity, bioavailability and bio-reactivity in fish intestinal cells. These results demonstrated that the luminal composition can affect the cells' metal bioavailability and bio-reactivity while also changing the overall toxicity of the metal itself. Classic medium components, such as Cl and Ca which have a protective nature for metals, were shown to influence toxicity of divalent metals such as cadmium and zinc but not of silver and copper. This study shows that metal complexes can be bioavailable and toxic and suggests that models like the FIAM and BLM are not appropriate to predict toxicity of metals in brackish and seawater where these complexes can form and be absorbed by the intestine of fish. Conversely, other medium components, not traditionally seen as important for the gill such as HCO_3^-, were much more influential in the RTgutGC intestinal model inducing an increase in silver, cadmium and zinc bio-reactivity. More studies are necessary to elucidate the complete scope of luminal juice composition on metal exposure, and other important intestinal physiology processes (i.e. pH, enzymatic composition and activity, etc.) need to be incorporated into this method.

REFERENCES

Allen, H.E., Hall, R.H., Brisbin, T.D., 1980. Metal speciation. Effects on aquatic toxicity. Environ Sci Technol 14, 441-443.

Ando, M., Subramanyam, V., 1990. Bicarbonate Transport Systems in the Intestine of the Seawater Eel.

Andrews, G.K., 2001. Cellular zinc sensors: MTF-1 regulation of gene expression. Biometals 14, 223-237.

Antony Jesu Prabhu, P., Stewart, T., Silva, M., Amlund, H., Ørnsrud, R., Lock, E.J., Waagbo, R., Hogstrand, C., 2018. Zinc uptake in fish intestinal epithelial model RTgutGC: Impact of media ion composition and methionine chelation. Journal of Trace Elements in Medicine and Biology 50, 377-383.

Apines-Amar, M.J.S., Satoh, S., Caipang, C.M.A., Kiron, V., Watanabe, T., Aoki, T., 2004. Amino acid-chelate: a better source of Zn, Mn and Cu for rainbow trout, Oncorhynchus mykiss. Aquaculture 240, 345-358.

Bielmyer, G.K., Brix, K.V., Grosell, M., 2008. Is Cl- protection against silver toxicity due to chemical speciation? Aquat Toxicol 87, 81-87.

Bucking, C., Wood, C.M., 2006. Gastrointestinal processing of Na+, Cl-, and K+ during digestion: implications for homeostatic balance in freshwater rainbow trout. Am J Physiol Regul Integr Comp Physiol 291, R1764-1772.

Burke, J., Handy, R.D., 2005. Sodium-sensitive and -insensitive copper accumulation by isolated intestinal cells of rainbow trout Oncorhynchus mykiss. J Exp Biol 208, 391-407.

Bury, N.R., Walker, P.A., Glover, C.N., 2003. Nutritive metal uptake in teleost fish. J Exp Biol 206, 11-23.

Campbell, P.G., Stokes, P.M., 1985. Acidification and toxicity of metals to aquatic biota. Canadian Journal of Fisheries and Aquatic Sciences 42, 2034-2049.

Coyle, P., Philcox, J.C., Carey, L.C., Rofe, A.M., 2002. Metallothionein: the multipurpose protein. Cell Mol Life Sci 59, 627-647.

Franklin, N.M., Glover, C.N., Nicol, J.A., Wood, C.M., 2005. Calcium Cadmium Interactions at Uptake Surfaces in Rainbow Trout. Environmental Toxicology and Chemistry 24, 2954-2964.

Gadagkar, S.R., Call, G.B., 2015. Computational tools for fitting the Hill equation to dose-response curves. J Pharmacol Toxicol Methods 71, 68-76.

Giles, N.M., Giles, G.I., Jacob, C., 2003. Multiple roles of cysteine in biocatalysis. Biochem Biophys Res Commun 300, 1-4.

Grosell, M., Blanchard, J., Brix, K.V., Gerdes, R., 2007. Physiology is pivotal for interactions between salinity and acute copper toxicity to fish and invertebrates. Aquat Toxicol 84, 162-172.

Grosell, M., Taylor, J.R., 2007. Intestinal anion exchange in teleost water balance. Comp Biochem Physiol A Mol Integr Physiol 148, 14-22.

Grosell, M., Wood, C.M., Wilson, R.W., Bury, N.R., Hogstrand, C., Rankin, C., Jensen, F.B., 2005. Bicarbonate secretion plays a role in chloride and water absorption of the European flounder intestine. Am J Physiol Regul Integr Comp Physiol 288, R936-946.

Gunther, V., Lindert, U., Schaffner, W., 2012. The taste of heavy metals: gene regulation by MTF-1. Biochim Biophys Acta 1823, 1416-1425.

Gustafsson, J.P., 2013. Visual Minteq 3.1.

Handy, R.D., Eddy, F.B., Baines, H., 2002. Sodium-dependent copper uptake across epithelia: a review of rationale with experimental evidence from gill and intestine. Biochim Biophys Acta 1566, 104-115.

Handy, R.D., Musonda, M.M., Phillips, C., Falla, S.J., 2000. Mechanisms of gastrointestinal copper absorption in the African walking catfish: copper dose-effects and a novel anion-dependent pathway in the intestine. J Exp Biol 203, 2365-2377.

Hardyman, J.E., Tyson, J., Jackson, K.A., Aldridge, C., Cockell, S.J., Wakeling, L.A., Valentine, R.A., Ford, D., 2016. Zinc sensing by metal-responsive transcription factor 1 (MTF1) controls metallothionein and ZnT1 expression to buffer the sensitivity of the transcriptome response to zinc. Metallomics 8, 337-343.

Hoch, E., Lin, W., Chai, J., Hershfinkel, M., Fu, D., Sekler, I., 2012. Histidine pairing at the metal transport site of mammalian ZnT transporters controls Zn2+ over Cd2+ selectivity. Proc Natl Acad Sci U S A 109, 7202-7207.

Ibrahim, M., Oldham, D., Minghetti, M., 2020. Role of metal speciation in the exposure medium on the toxicity, bioavailability and bio-reactivity of copper, silver, cadmium and

zinc in the rainbow trout gut cell line (RTgutGC). Comp Biochem Physiol C Toxicol Pharmacol 236, 108816.

Kamunde, C., Grosell, M., Higgs, D., Wood, C.M., 2002. Copper metabolism in actively growing rainbow trout (Oncorhynchus mykiss): interactions between dietary and waterborne copper uptake. The Journal of Experimental Biology 205, 279–290.

Kurita, Y., Nakada, T., Kato, A., Doi, H., Mistry, A.C., Chang, M.H., Romero, M.F., Hirose, S., 2008. Identification of intestinal bicarbonate transporters involved in formation of carbonate precipitates to stimulate water absorption in marine teleost fish. Am J Physiol Regul Integr Comp Physiol 294, R1402-1412.

Liu, Z., Li, H., Soleimani, M., Girijashanker, K., Reed, J.M., He, L., Dalton, T.P., Nebert, D.W., 2008. Cd2+ versus Zn2+ uptake by the ZIP8 HCO3--dependent symporter: kinetics, electrogenicity and trafficking. Biochem Biophys Res Commun 365, 814-820.

Maage, A., KJulshamn, K., Berge, G.E., 2001. Zinc gluconate and zinc sulphate as dietary zinc sources for

Atlantic salmon. Aquaculture Nutrition 7.

Martinez-Finley, E.J., Chakraborty, S., Fretham, S.J., Aschner, M., 2012. Cellular transport and homeostasis of essential and nonessential metals. Metallomics 4, 593-605.

Matson, C.W., Bone, A.J., Auffan, M., Lindberg, T.T., Arnold, M.C., Hsu-Kim, H., Wiesner, M.R., Di Giulio, R.T., 2016. Silver toxicity across salinity gradients: the role of dissolved silver chloride species (AgCl x) in Atlantic killifish (Fundulus heteroclitus) and medaka (Oryzias latipes) early life-stage toxicity. Ecotoxicology 25, 1105-1118.

Mbah, A.K., Paothong, A., 2014. Shapiro–Francia test compared to other normality test using expectedp-value. Journal of Statistical Computation and Simulation 85, 3002-3016.

McNaught, A.D., Wilkinson, A., International Union of Pure and Applied Chemistry., 1997. Compendium of chemical terminology : IUPAC recommendations, 2nd ed. Blackwell Science, Oxford England ; Malden, MA, USA.

McRae, N.K., Gaw, S., Glover, C.N., 2016. Mechanisms of zinc toxicity in the galaxiid fish, Galaxias maculatus. Comp Biochem Physiol C Toxicol Pharmacol 179, 184-190.

Minghetti, M., Dudefoi, W., Ma, Q., Catalano, J.G., 2019. Emerging investigator series: linking chemical transformations of silver and silver nanoparticles in the extracellular and intracellular environments to their bio-reactivity. Environmental Science: Nano 6, 2948-2957.

Minghetti, M., Leaver, M.J., Carpene, E., George, S.G., 2008. Copper transporter 1, metallothionein and glutathione reductase genes are differentially expressed in tissues of sea bream (Sparus aurata) after exposure to dietary or waterborne copper. Comp Biochem Physiol C Toxicol Pharmacol 147, 450-459.

Minghetti, M., Schirmer, K., 2016. Effect of media composition on bioavailability and toxicity of silver and silver nanoparticles in fish intestinal cells (RTgutGC). Nanotoxicology 10, 1526-1534.

Minghetti, M., Schnell, S., Chadwick, M.A., Hogstrand, C., Bury, N.R., 2014. A primary FIsh Gill Cell System (FIGCS) for environmental monitoring of river waters. Aquat Toxicol 154, 184-192.

Morcillo, P., Esteban, M.A., Cuesta, A., 2016. Heavy metals produce toxicity, oxidative stress and apoptosis in the marine teleost fish SAF-1 cell line. Chemosphere 144, 225-233.

Morgan, T.P., Grosell, M., Gilmour, K.M., Playle, R.C., Wood, C.M., 2004. Time course analysis of the mechanism by which silver inhibits active Na and Cl uptake in gills of rainbow trout. Am J Physiol Regul Integr Comp Physiol 287, 234-342.

Nebert, D.W., Galvez-Peralta, M., Hay, E.B., Li, H., Johansson, E., Yin, C., Wang, B., He, L., Soleimani, M., 2012. ZIP14 and ZIP8 zinc/bicarbonate symporters in Xenopus oocytes: characterization of metal uptake and inhibition. Metallomics 4, 1218-1225.

Niyogi, S., Wood, C.M., 2004. Biotic ligand model, a flexible tool for developing site-specific water quality guidelines for metals. Environ Sci Technol 38, 6177-6192.

Ojo, A.A., Wood, C.M., 2007. In vitro analysis of the bioavailability of six metals via the gastro-intestinal tract of the rainbow trout (Oncorhynchus mykiss). Aquat Toxicol 83, 10-23.

Ojo, A.A., Wood, C.M., 2008. In vitro characterization of cadmium and zinc uptake via the gastro-intestinal tract of the rainbow trout (Oncorhynchus mykiss): Interactive effects and the influence of calcium. Aquat Toxicol 89, 55-64.

Paquin, P.R., Gorsuch, J.W., Apte, S., Batley, G.E., Bowles, K.C., Campbell, P.G., Delos, C.G., Di Toro, D.M., Dwyer, R.L., Galvez, F., Gensemer, R.W., Goss, G.G., Hostrand, C., Janssen, C.R., McGeer, J.C., Naddy, R.B., Playle, R.C., Santore, R.C., Schneider, U., Stubblefield, W.A., Wood, C.M., Wu, K.B., 2002. The biotic ligand model: a historical overview. Comp Biochem Physiol C Toxicol Pharmacol 133, 3-35.

Parra-Frutos, I., 2012. Testing homogeneity of variances with unequal sample sizes. Computational Statistics 28, 1269-1297.

Pont, G.D., Domingos, F.X., Fernandes-de-Castilho, M., Val, A.L., 2017. Potential of the Biotic Ligand Model (BLM) to Predict Copper Toxicity in the White-Water of the Solimoes-Amazon River. Bull Environ Contam Toxicol 98, 27-32.

Reiley, M.C., 2007. Science, policy, and trends of metals risk assessment at EPA: how understanding metals bioavailability has changed metals risk assessment at US EPA. Aquat Toxicol 84, 292-298.

Schirmer, K., Chan, A.G., Greenberg, B.M., Dixon, D.G., Bols, N.C., 1997. Methodology for demonstrating and measuring the photocytotoxicity of fluoranthene to fish cells in culture. Toxicol In Vitro 11, 107-119.

Scott, G.R., Schulte, P.M., Wood, C.M., 2006. Plasticity of osmoregulatory function in the killifish intestine: drinking rates, salt and water transport, and gene expression after freshwater transfer. J Exp Biol 209, 4040-4050.

Shehadeh, Z.H., Gordon, M.S., 1969. The role of the intestine in salinity adaptation of the rainbow trout, *salmo gairdneri*. Comp Biochem Physiol 30, 197 - 418.

Smith, K.S., Balistrieri, L.S., Todd, A.S., 2015. Using biotic ligand models to predict metal toxicity in mineralized systems. Applied Geochemistry 57, 55-72.

Thevenod, F., Fels, J., Lee, W.K., Zarbock, R., 2019. Channels, transporters and receptors for cadmium and cadmium complexes in eukaryotic cells: myths and facts. Biometals.

van der Oost, R., Beyer, J., Vermeulen, N.P., 2003. Fish bioaccumulation and biomarkers in environmental risk assessment: a review. Environ Toxicol Pharmacol 13, 57-149.

Vercauteren, K., Blust, R., 1996. Bioavailability of dissolved zinc to the common mussel Mytilus edulis in complexing environments. Marine Ecology Progress Series 137, 123-132.

Walker, P.A., Kille, P., Hurley, A., Bury, N.R., Hogstrand, C., 2008. An in vitro method to assess toxicity of waterborne metals to fish. Toxicol Appl Pharmacol 230, 67-77.

Wang, J., Zhu, X., Huang, X., Gu, L., Chen, Y., Yang, Z., 2016. Combined effects of cadmium and salinity on juvenile Takifugu obscurus: cadmium moderates salinity tolerance; salinity decreases the toxicity of cadmium. Sci Rep 6, 30968.

Wood, C.M., Grosell, M., Hogstrand, C., H., H., 2002. Kinetics of radiolabelled silver uptake and depuration in the gills of rainbow trout (*Oncorhynchus mykiss*) and European eel (*Anguilla anguilla*): the influence of silver speciation. Aquatic Toxicology 56, 197-213.

Zheng, D., Feeney, G.P., Kille, P., Hogstrand, C., 2008. Regulation of ZIP and ZnT zinc transporters in zebrafish gill: zinc repression of ZIP10 transcription by an intronic MRE cluster. Physiol Genomics 34, 205-214.

Zimnicka, A.M., Ivy, K., Kaplan, J.H., 2011. Acquisition of dietary copper: a role for anion transporters in intestinal apical copper uptake. Am J Physiol Cell Physiol 300, C588-599.

APPENDICES

Tables

Table 1: Composition of the six experimental exposure media used for metal exposures in RTgutGC bioassays. Media components changed were Cl^{-1}, Ca^{2+}, PO_4^{-3}, CO_3^{-1}, and Cys. Medium component values are nominal concentrations (mM), osmolality is in milliosmole per kg ($mOsm*kg^{-1}$) and ionic strength is presented as millimole per kg ($mmol*kg^{-1}$). pH and osmolality were measured via pH meter and osmometer, respectively. Ionic strength was calculated using Visual Minteq.

Component (mM)	Ex	Cl_{Low}	Cl_{Low}-Ca_{Low}	P_{Free}	HCO_3^-	Cys
Cl^{-1}	168.80	1.00	1.00	158.30	158.30	168.80
Ca^{+2}	1.40	1.50	0.08	1.20	1.20	1.40
Mg^{+2}	4.30	3.80	3.80	4.30	4.30	4.30
Na^{+1}	163.80	159.00	159.00	162.00	162.00	163.80
K^{+1}	6.60	6.10	6.10	6.00	6.00	6.60
PO_4^{-3}	1.80	1.80	1.80	0.00	0.00	1.80
SO_4^{-2}	1.90	1.90	1.90	1.90	1.90	1.90
HEPES	0.00	0.00	0.00	15.00	10.00	0.00
CO_3^{-2}	0.00	0.00	0.00	0.00	5.00	0.00
NO_3^{-1}	0.00	164.00	164.00	0.00	0.00	0.00
pH	7.04	7.05	7.03	7.11	7.40	7.04
Osmolality ($mOsm*kg^{-1}$)	347.67	325.86	330.09	334.00	335.30	347.67
Ionic Strength ($mmol*kg^{-1}$)	176.00	177.30	150.50	167.60	167.50	176.20

Table 2: Top two dominant species and free metal ion percentage in each metal in respective media. Values are percentage of total metal in solution. Percentages are calculated using Visual Minteq added at a metal concentration equal to 200 μM at 19 ºC and pH set to each medium's respective measured pH (Table 1).

	Ag	Cd	Cu	Zn
L15/ex	$AgCl_2^{-2}$: 75.6% $AgCl_3^{-2}$: 19.1% Ag+: 0.03%	$CdCl^+$: 60.6% Cd^{+2}: 12.4%	Cu^{+2}: 41.6% $CuPO_{4(aq)}$: 38.7%	Zn^{+2}: 74.3% $ZnCl^+$: 11.0%
Cl_{Low}	Ag^{+1}: 47.2% $AgCl_{(aq)}$: 45.9%	Cd^{+2}: 61.5% $CdHPO_{4\ (aq)}$: 22.5%	Cu^{+2}: 40.0% $CuHPO_{4\ (aq)}$: 38.7%	Zn^{+2}: 74.3% $ZnHPO_{4\ (aq)}$: 11.2%
Cl_{Low}-Ca_{Low}	Ag^{+1}: 47.4% $AgCl_{(aq)}$: 45.0%	Cd^{+2}: 59.6% $CdHPO_{4\ (aq)}$: 24.6%	$CuHPO_{4\ (aq)}$: 35.8% Cu^{+2}: 33.4%	Zn^{+2}: 73.0% $ZnHPO_{4\ (aq)}$: 12.4%
P_{Free}	$AgCl_2^-$: 77.6% $AgCl_3^{-2}$: 15.8% Ag^+: 0.04%	$CdCl^+$: 64.6% $CdCl_{2\ (aq)}$: 20.0% Cd^{+2}: 15.17%	Cu^{+2}: 35.0% $Cu_3(OH)_4^{+2}$: 23.6%	Zn^{+2}: 85.8% $ZnCl^+$: 11.0%
HCO_3^-	$AgCl_2^-$: 77.6% $AgCl_3^{-2}$: 15.8% Ag^+: 0.04%	$CdCl^+$: 64.0% $CdCl_{2\ (aq)}$: 19.9% Cd^{+2}: 15.04%	$CuCO_{3\ (aq)}$: 63.0% Cu^{+2}: 25.6%	Zn^{+2}: 81.4% $ZnCl^+$: 10.5%
Cys	Ag_2Cys: 98.5% Ag_2Cys^-: 0.4% Ag^+: 0.00%	$CdCys^0$: 53.5% $CdCys^-$: 35.2% Cd^{+2}: 0.00%	$CuCys^-$: 59.8% $CuCys^0$: 40.2% Cu^{+2}: 0.00%	$ZnCys^-$: 90.7% $ZnCys^0$: 1.8% Zn^{+2}: 2.55%

Table 3: Solubility of $AgNO_3$ (A), $CdCl_2$ (B), $CuSO_4$ (C), and $ZnSO_4$ (D) in all of the media. Values represent percentage of the metal concentration (µM) dissolved in solution, calculated by Visual Minteq. Solid phase metal species consisted of cerargyrite for Ag in all media, and $Cd_3(PO_4)_2$ for Cd in low Cl^- media. Copper precipitated as $Cu_3(PO_4)_2$ in L-15/ex, L-15/$Cl_{Low,}$ L-15/Cl_{Low}-Ca_{Low} and L-15/Cys, as brochantite in L-15/P_{Free} and Azurite in L-15/HCO_3^-. Zinc precipitated as $Zn_3(PO_4)_2$:$4H_2O$ in L-15/ex, L-15/$Cl_{Low,}$ L-15/Cl_{Low}-Ca_{Low} and L-15/Cys, and Hydrozincite in L-15/P_{Free} and Azurite in L-15/HCO_3^-.

A $AgNO_3$ µM	L-15/ex % Dissolved	Cl_{Low} % Dissolved	Cl_{Low}-Ca_{Low} % Dissolved	P_{Free} % Dissolved	HCO_3^- % Dissolved	Cys % Dissolved
200	2.3	0.2	0.2	1.8	1.8	100.0
40	11.5	1.1	1.1	9.2	9.2	100.0
20	23.1	2.2	2.3	18.4	18.4	100.0
9	51.3	5.0	5.0	40.8	40.8	100.0
7	66.0	6.5	6.4	52.4	52.5	100.0
5	92.6	8.6	9.0	73.4	73.4	100.0
4.7	98.3	9.2	9.6	78.1	78.1	100.0
4.6	100.0	9.4	9.8	79.8	79.8	100.0
3.7	100.0	11.6	12.2	99.2	99.3	100.0
3.6	100.0	12.0	12.5	100.0	100.0	100.0
0.9	100.0	47.8	50.0	100.0	100.0	100.0
0.5	100.0	86.1	90.0	100.0	100.0	100.0
0.45	100.0	95.7	100.0	100.0	100.0	100.0
0.4	100.0	100.0	100.0	100.0	100.0	100.0
0.1	100.0	100.0	100.0	100.0	100.0	100.0

Table 3 (continued): Dissolution of $AgNO_3$ (A), $CdCl_2$ (B), $CuSO_4$ (C), and $ZnSO_4$ (D) in all of the media.

B CdCl2 µM	L-15/ex % Dissolved	Cl_{Low} % Dissolved	Cl_{Low}-Ca_{Low} % Dissolved	P_{Free} % Dissolved	HCO_3^- % Dissolved	Cys % Dissolved
200	100.0	34.1	33.8	100.0	100.0	100.0
150	100.0	45.2	44.6	100.0	100.0	100.0
100	100.0	67.1	66.3	100.0	100.0	100.0
84	100.0	79.8	78.7	100.0	100.0	100.0
83.5	100.0	80.3	79.2	100.0	100.0	100.0
73.5	100.0	91.1	89.8	100.0	100.0	100.0
73	100.0	91.8	90.3	100.0	100.0	100.0
67.5	100.0	98.8	99.0	100.0	100.0	100.0
67	100.0	100.0	100.0	100.0	100.0	100.0
40	100.0	100.0	100.0	100.0	100.0	100.0
20	100.0	100.0	100.0	100.0	100.0	100.0
5	100.0	100.0	100.0	100.0	100.0	100.0
0.5	100.0	100.0	100.0	100.0	100.0	100.0
0.1	100.0	100.0	100.0	100.0	100.0	100.0

Table 3 (continued): Dissolution of $AgNO_3$ (A), $CdCl_2$ (B), $CuSO_4$ (C), and $ZnSO_4$ (D) in all of the media.

C $CuSO_4$ µM	L-15/ex % Dissolved	Cl_{Low} % Dissolved	Cl_{Low}-Ca_{Low} % Dissolved	P_{Free} % Dissolved	HCO_3^- % Dissolved	Cys % Dissolved
200	1.6	1.9	1.8	0.9	0.6	1.6
10	31.1	38.2	35.0	17.5	11.7	31.1
6.5	47.9	58.7	53.8	27.0	18.0	47.9
4	77.8	95.4	87.3	43.8	29.2	77.8
3.855	80.7	99.0	90.6	45.4	30.3	80.7
3.8	81.9	100.0	91.9	46.1	30.8	81.9
3.13	99.4	100.0	100.0	56.0	37.4	99.4
3.1	100.0	100.0	100.0	56.5	37.7	100.0
2.45	100.0	100.0	100.0	71.5	47.7	100.0
2.4	100.0	100.0	100.0	73.0	48.7	100.0
2.1	100.0	100.0	100.0	83.4	55.7	100.0
1.77	100.0	100.0	100.0	99.0	66.1	100.0
1.7	100.0	100.0	100.0	100.0	68.8	100.0
1.4	100.0	100.0	100.0	100.0	83.5	100.0
1.35	100.0	100.0	100.0	100.0	86.6	100.0
1.18	100.0	100.0	100.0	100.0	99.1	100.0
1.15	100.0	100.0	100.0	100.0	100.0	100.0

Table 3 (continued): Dissolution of AgNO3 (A), CdCl2 (B), CuSO4 (C), and ZnSO4 (D) in all of the media.

D	L-15/ex	Cl_{Low}	Cl_{Low}-Ca_{Low}	P_{Free}	HCO_3^-	Cys
$ZnSO_4$ µM	% Dissolved	% Dissolved	% Dissolved	% Dissolved	% Dissolved	% Dissolved
500	1.3	1.5	1.4	100.0	3.1	39.1
200	2.9	3.6	3.2	100.0	7.4	96.6
150	3.9	4.7	4.2	100.0	9.8	100.0
135	4.3	5.3	4.7	100.0	10.8	100.0
132	4.4	5.4	4.8	100.0	11.0	100.0
131.9	4.4	5.4	4.8	100.0	11.1	100.0
109	5.3	6.5	5.8	100.0	13.3	100.0
108	5.3	6.5	5.8	100.0	13.4	100.0
100	5.8	7.0	6.3	100.0	14.4	100.0
50	11.4	13.8	12.5	100.0	28.7	100.0
25	22.7	27.8	24.8	100.0	57.1	100.0
18	31.5	38.5	34.4	100.0	79.2	100.0
17.4	32.6	39.8	35.7	100.0	81.9	100.0
17.3	32.8	40.1	35.9	100.0	82.4	100.0
14.3	40.7	48.4	43.4	100.0	99.6	100.0
14.2	41.0	48.8	43.6	100.0	100.0	100.0
10	56.6	69.2	51.5	100.0	100.0	100.0
9	62.9	76.9	61.8	100.0	100.0	100.0
8.9	63.6	77.7	69.7	100.0	100.0	100.0
8.8	64.3	78.6	70.5	100.0	100.0	100.0
7.5	75.5	92.2	82.7	100.0	100.0	100.0
6	94.3	98.8	82.4	100.0	100.0	100.0
5.7	99.3	100.0	99.6	100.0	100.0	100.0
5.5	100.0	100.0	100.0	100.0	100.0	100.0

Table 4: Exposure concentrations of each metal for cytotoxicity experiments. Metal exposures reported are nominal μM concentrations.

Exposure Concentrations (μM)	Ag	Cd	Cu	Zn
Dose 1	50	200	200	500
Dose 2	10	40	40	100
Dose 3	2	20	20	50
Dose 4	1	5	5	25
Dose 5	0.4	0.5	0.5	5
Dose 6	0.08	0.1	0.1	1

Table 5: Percent recovery of metals in stock and exposure solutions. Stock solutions were dissolved in ultrapure H_2O. Measurements done using ICP-OES.

% recovery	Ag	Cd	Cu	Zn
Stock	104.8	98.4	100.5	102.4
Ex	109.2	93.1	104.5	107.3
Cl_{Low}-Ca_{Low}	105.9	93.0	97.9	106.5
P_{Free}	89.9	91.1	93.0	104.5
HCO_3^-	106.9	91.9	93.3	107.6
Cys	97.9	92.3	91.8	109.3

Table 6: EC_{50} values (in µM) calculated exposing RTgutGC to silver, cadmium, copper, and zinc for 24 hours. Values are mean ± SD from at least 3 independent experiments (n = 3-12). Different Latin letters indicate significant difference in metal toxicity between the media within each endpoint and the geomean ($p < 0.05$; One-way ANOVA; Tukey post hoc). Geomean is the geometric mean of all three endpoints. Greek letters indicate difference in the geomean metal toxicity hierarchy within a media, where $\alpha > \beta > \gamma > \delta$ ($p < 0.05$; One-way ANOVA; Tukey post hoc).

Ag	Metabolic Activity	Membrane Integrity	Lysosome integrity	Geomean
L-15/ex	1.42 ± 0.28^{AB}	2.10 ± 0.20^{A}	2.05 ± 0.58^{A}	$1.77 \pm 0.30^{A\ \alpha}$
Cl_{Low}	1.16 ± 0.22^{B}	2.50 ± 1.36^{A}	1.41 ± 0.36^{A}	$1.54 \pm 0.51^{A\ \alpha}$
Cl_{Low}-Ca_{Low}	1.17 ± 0.22^{B}	1.66 ± 0.27^{A}	1.96 ± 1.30^{A}	$1.59 \pm 0.52^{A\ \alpha}$
P_{Free}	1.52 ± 0.14^{AB}	2.15 ± 0.24^{A}	4.32 ± 2.92^{A}	$2.64 \pm 0.61^{A\ \alpha}$
HCO_3^-	1.84 ± 0.18^{A}	2.41 ± 0.29^{A}	4.51 ± 2.62^{A}	$2.34 \pm 0.60^{A\ \alpha}$

Cd	Metabolic Activity	Membrane Integrity	Lysosome integrity	Geomean
L-15/ex	39.57 ± 24.61^{A}	42.44 ± 15.07^{B}	34.27 ± 5.90^{A}	$37.60 \pm 8.34^{A\ \gamma}$
Cl_{Low}	21.54 ± 5.44^{AB}	80.05 ± 20.01^{A}	13.95 ± 5.10^{BC}	$3.03 \pm 1.20^{BC\ \beta}$
Cl_{Low}-Ca_{Low}	2.39 ± 0.88^{C}	3.99 ± 1.84^{C}	3.00 ± 1.24^{C}	$28.30 \pm 4.67^{AB\ \gamma}$
P_{Free}	11.18 ± 4.88^{B}	28.21 ± 10.41^{BC}	16.95 ± 5.03^{B}	$9.77 \pm 1.82^{BC\ \alpha\beta}$
HCO_3^-	5.21 ± 0.80^{BC}	23.14 ± 4.43^{BC}	8.18 ± 3.82^{BC}	$17.41 \pm 6.17^{B\ \beta}$

Cu	Metabolic Activity	Membrane Integrity	Lysosome integrity	Geomean
L-15/ex	4.01 ± 1.35^{A}	8.65 ± 2.63^{A}	17.72 ± 1.81^{A}	$6.75 \pm 2.42^{A\ \beta}$
Cl_{Low}	3.66 ± 1.41^{A}	6.42 ± 1.96^{A}	6.44 ± 3.09^{B}	$3.16 \pm 0.49^{B\ \alpha}$
Cl_{Low}-Ca_{Low}	2.08 ± 1.29^{A}	5.18 ± 2.19^{A}	4.30 ± 3.28^{B}	$5.28 \pm 1.90^{AB\ \beta}$
P_{Free}	2.73 ± 0.75^{A}	4.80 ± 0.85^{A}	2.11 ± 1.05^{B}	$3.57 \pm 1.49^{AB\ \alpha}$
HCO_3^-	3.53 ± 0.61^{A}	6.70 ± 2.41^{A}	2.04 ± 1.42^{B}	$2.98 \pm 0.84^{B\ \alpha}$

Zn	Metabolic Activity	Membrane Integrity	Lysosome integrity	Geomean
L-15/ex	101.6 ± 28.35^{A}	132.72 ± 52.88^{A}	65.69 ± 15.57^{A}	$89.61 \pm 8.66^{A\ \delta}$
Cl_{Low}	60.49 ± 19.82^{AB}	95.13 ± 63.10^{AB}	36.89 ± 21.80^{AB}	$23.42 \pm 2.47^{B\ \gamma}$
Cl_{Low}-Ca_{Low}	15.64 ± 0.63^{BC}	25.98 ± 8.79^{B}	32.54 ± 0.67^{AB}	$57.13 \pm 23.59^{AB\ \gamma}$
P_{Free}	45.68 ± 4.77^{BC}	78.66 ± 28.64^{AB}	62.86 ± 11.77^{A}	$19.41 \pm 14.33^{C\ \beta}$
HCO_3^-	12.52 ± 8.14^{C}	36.34 ± 35.93^{B}	17.52 ± 12.55^{B}	$60.30 \pm 10.38^{AB\ \gamma}$

Table 7: Correlation of specific metal species and the geomean EC_{50} values. Geomean EC_{50} mean values were correlated with the calculated concentration percentage from Visual Minteq of the specific metal species (Table 2; Figure 1). Species not found in at least 3 media were removed from the calculation, and L-15/Cl_{Low}-Ca_{Low} was removed due to Ca not effecting speciation. Correlation was calculated using the Pearson R correlation coefficients ($p < 0.05$).

Metal	Species	p-value
Silver	Ag^{+}	0.3274
	$AgCl_{(aq)}$	0.3491
	$AgCl_2^{-}$	0.3095
	$AgCl_3^{-2}$	0.8832
Cadmium	Cd^{+2}	0.7761
	$CdCl^{+}$	0.6755
	$CdCl_{2\ (aq)}$	0.8396
Copper	Cu^{+2}	0.2641
	$CuCl^{+}$	0.8551
	$CuSO_{4\ (aq)}$	0.3804
Zinc	Zn^{+2}	0.5430
	$ZnCl^{+}$	0.9706
	$ZnSO_{4\ (aq)}$	0.7140

Table 8: Bioavailability of silver, cadmium, copper, and zinc in RTgutGC cells measure after a 24-hour exposure. Values are mean ± SD of ng of metal in cells seeded in 4 different wells (n = 4). Values are reported in ng of metal/mg of protein to account for variation in cell numbers. Different letters indicate significant difference between the media within each metal. Statistical analysis was performed via one-way ANOVA with a Tukey test post-hoc, $p < 0.05$.

ng metal per mg protein	Ag	Cd	Cu	Zn
Ex	632.3 ± 301.4^{A}	55.2 ± 16.3^{C}	47.1 ± 14.8^{B}	356.1 ± 63.7^{AB}
Cl_{Low}	90.3 ± 34.8^{B}	108.5 ± 11.7^{AB}	108.6 ± 21.0^{A}	102.7 ± 42.3^{C}
Cl_{Low}-Ca_{Low}	326.7 ± 179.5^{AB}	98.5 ± 11.5^{B}	41.1 ± 8.7^{B}	466.9 ± 60.5^{A}
HCO_3^{-}	678.4 ± 230.7^{A}	135.8 ± 13.7^{A}	41.8 ± 13.5^{B}	328.3 ± 53.8^{B}
Cys	189.8 ± 46.5^{B}	30.28 ± 8.3^{C}	38.8 ± 14.0^{B}	308.9 ± 64.1^{B}

Table 9: Primers used for the quantitative polymerase chain reaction (qPCR) used to determine metal bio-reactivity. Repository IDs are: MTb: M18104 NM_001124528; ZnT1: XM_021561788; GR: HF969248; EF1α: NM_001124339; Ubiquitin: NM_001124194 GenBank (http://www.ncbi.nim.nih.gov/).

Gene name	Forward primer 5'→3'	Reverse primer 5'→3'
MTb	GCTCTAAAACTGGCTCTTGC	GTCTAGGCTCAAGATGGTAC
ZnT1	TGGATCCGGGCTGAGGTGATGG	CAAGCACAGCCCGAGGAGGTTG
GR	TACACCGCGCCTCATATCCTCATT	TGCCAGCCATTTCCACAGC
EF1α	ATATCCGTCGTGGCAACGTGGC	TGAGCTCGCTGAACTTGCAGGC
Ubiquitin	GCTGCGTCTTCGTGGAGGCATT	TTGGGGCGCAGGTTGTTTGTGT

Figures

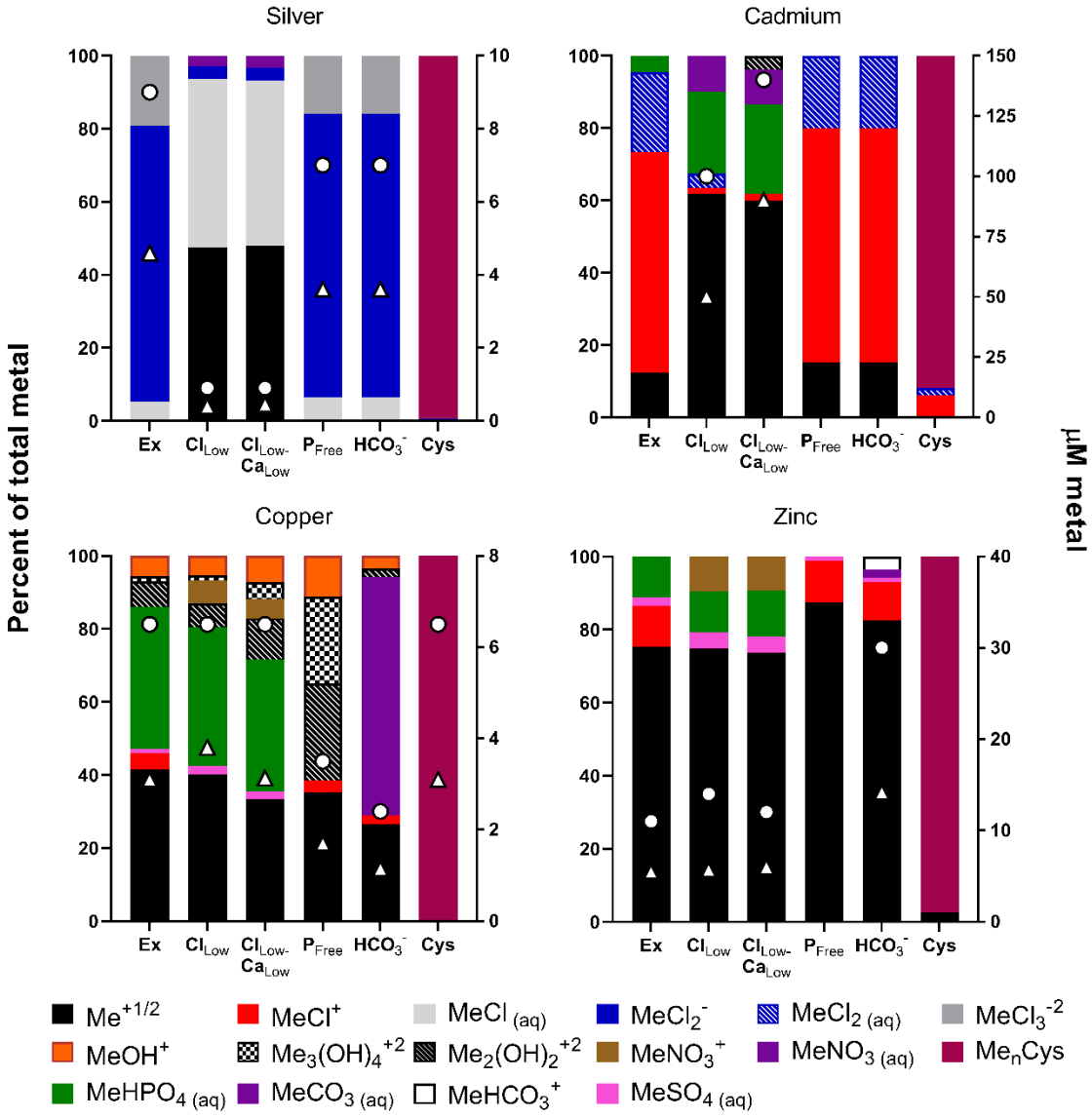

Figure 1: Metal speciation and precipitation in the exposure media calculated with Visual Minteq, at a concentration of 200 µM. Left Y-axis: speciation represented as percentage of total dissolved species. Species accounting for <1% are removed for graph clarity. Metal speciation % values are reported also in Table 2. Right Y-axis: metal concentration (in µM) at which 1% (triangles) and 50% (circles) is precipitated. Missing shapes represent 100% dissolution of metal at <200 µM. Metals used for calculation were $AgNO_3$, $CdCl_2$, $CuSO_4$, and $ZnSO_4$ in each media (Table 1). All the precipitation values are also reported in Figure 3.

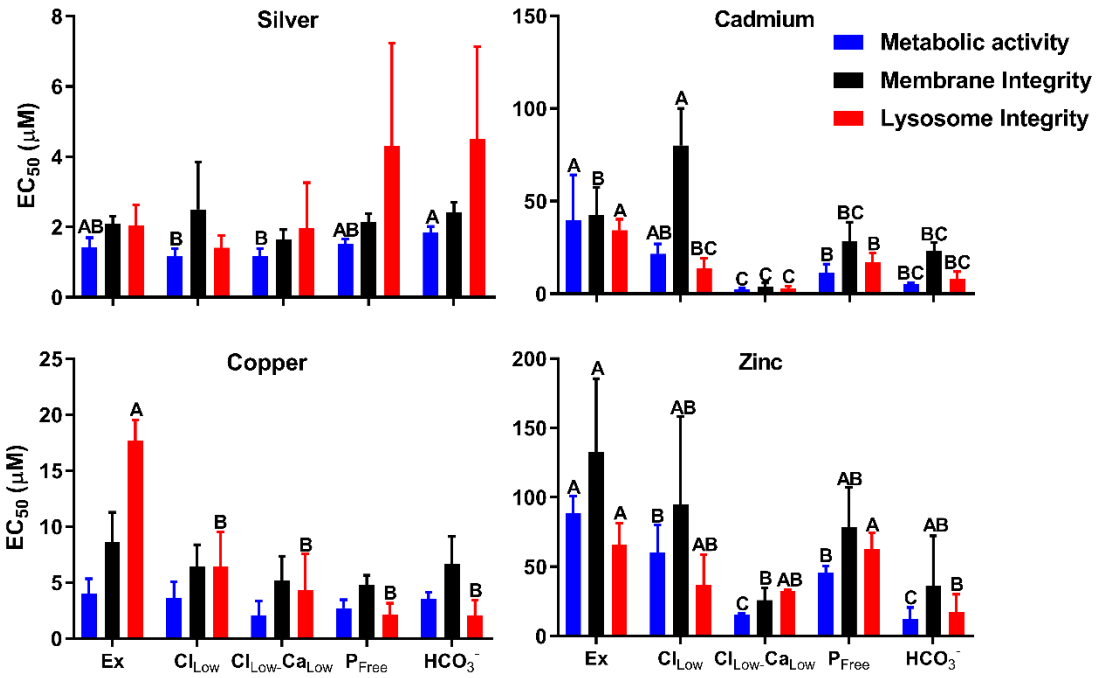

Figure 2: Mean EC_{50} ± SD from at least three independent experiments. EC_{50} values were calculated exposing RTgutGC cells to Ag, Cu, Zn, and Cd for 24 h in the indicated media. Bars bearing different letters are significantly different than other bars in same endpoint category (one-way ANOVA with a Tukey post-hoc test, $p < 0.05$, n=3-12). EC50s were determined using the dose response curves shown in Figure 4 using the non-linear regression sigmoidal dose-response curve fitting module using the Hill slope equation.

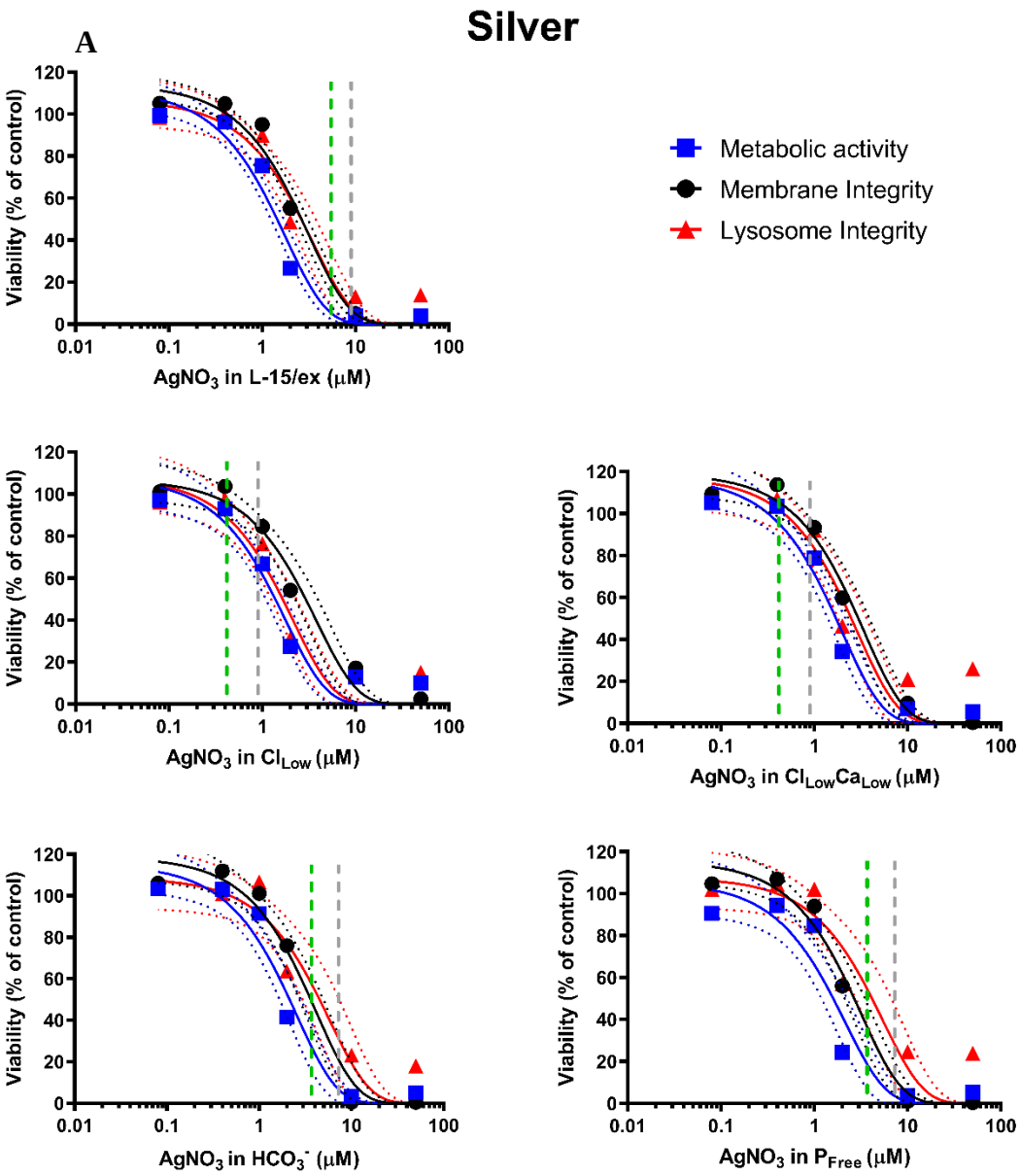

Figure 3A: Dose response curves for silver toxicity in RTgutGC cell viability exposed to silver for 24 hours in five different culture media differing in selected compontes (see Table 1). Viability is reported as percent of control (i.e. unexposed cells). Values shown are averages and dashed line represent 95% confidence interval of 3-12 independent experiments (n= 3-12). Solid lines represent the fitted curve. Vertical dashed lines show precipitation of metal (green = ~1% precipitation; grey = ~50% precipitation).

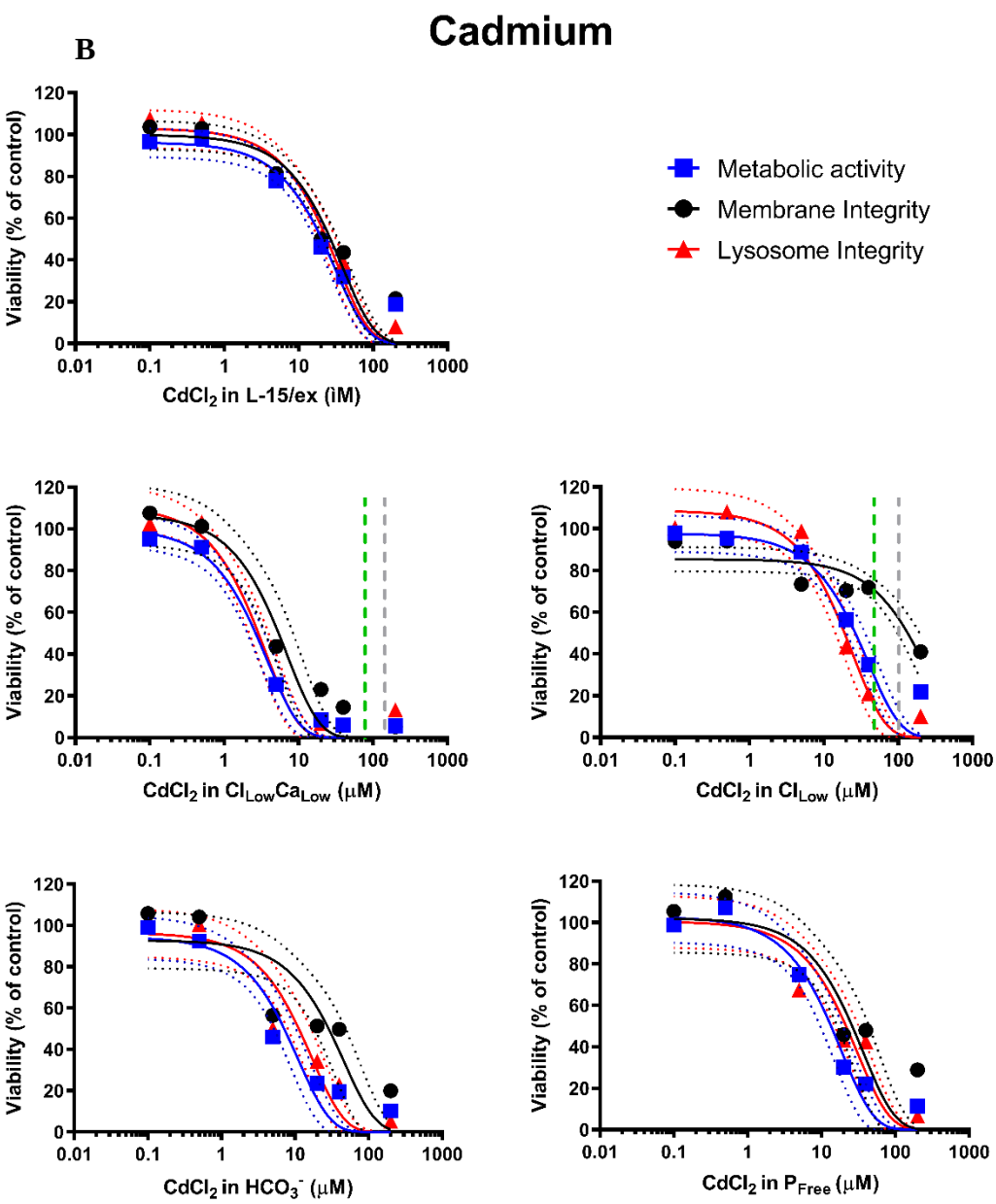

Figure 3B: Dose response curves for cadmium toxicity in RTgutGC cell viability exposed to cadmium for 24 hours in five different culture media differing in selected compontes (see Table 1). Viability is reported as percent of control (i.e. unexposed cells). Values shown are averages and dashed line represent 95% confidence interval of 3-12 independent experiments (n= 3-12). Solid lines represent the fitted curve. Vertical dashed lines show precipitation of metal (green = ~1% precipitation; grey = ~50% precipitation).

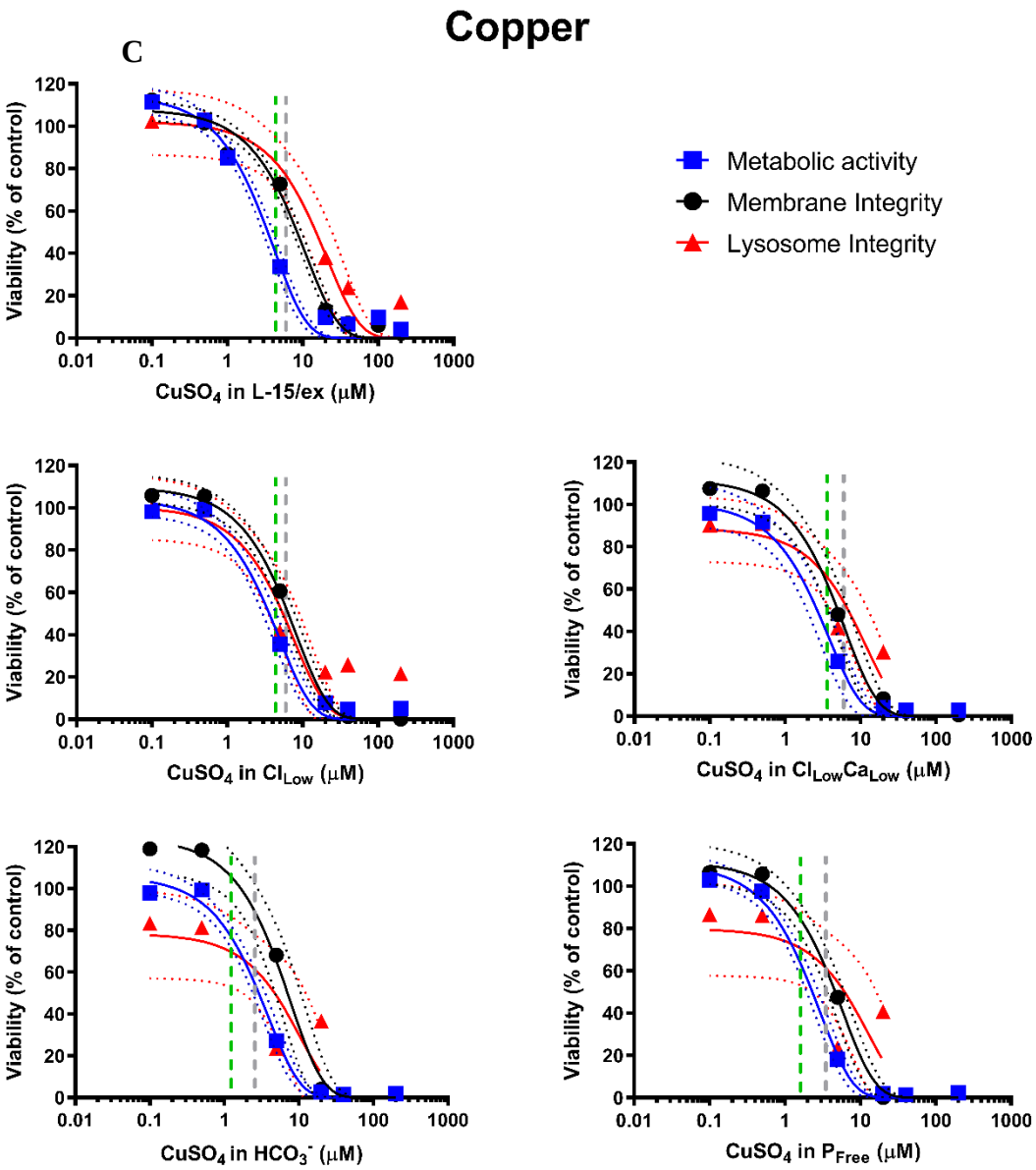

Figure 3C: Dose response curves for copper toxicity in RTgutGC cell viability exposed to copper for 24 hours in five different culture media differing in selected compontes (see Table 1). Viability is reported as percent of control (i.e. unexposed cells). Values shown are averages and dashed line represent 95% confidence interval of 3-12 independent experiments (n= 3-12). Solid lines represent the fitted curve. Vertical dashed lines show precipitation of metal (green = ~1% precipitation; grey = ~50% precipitation).

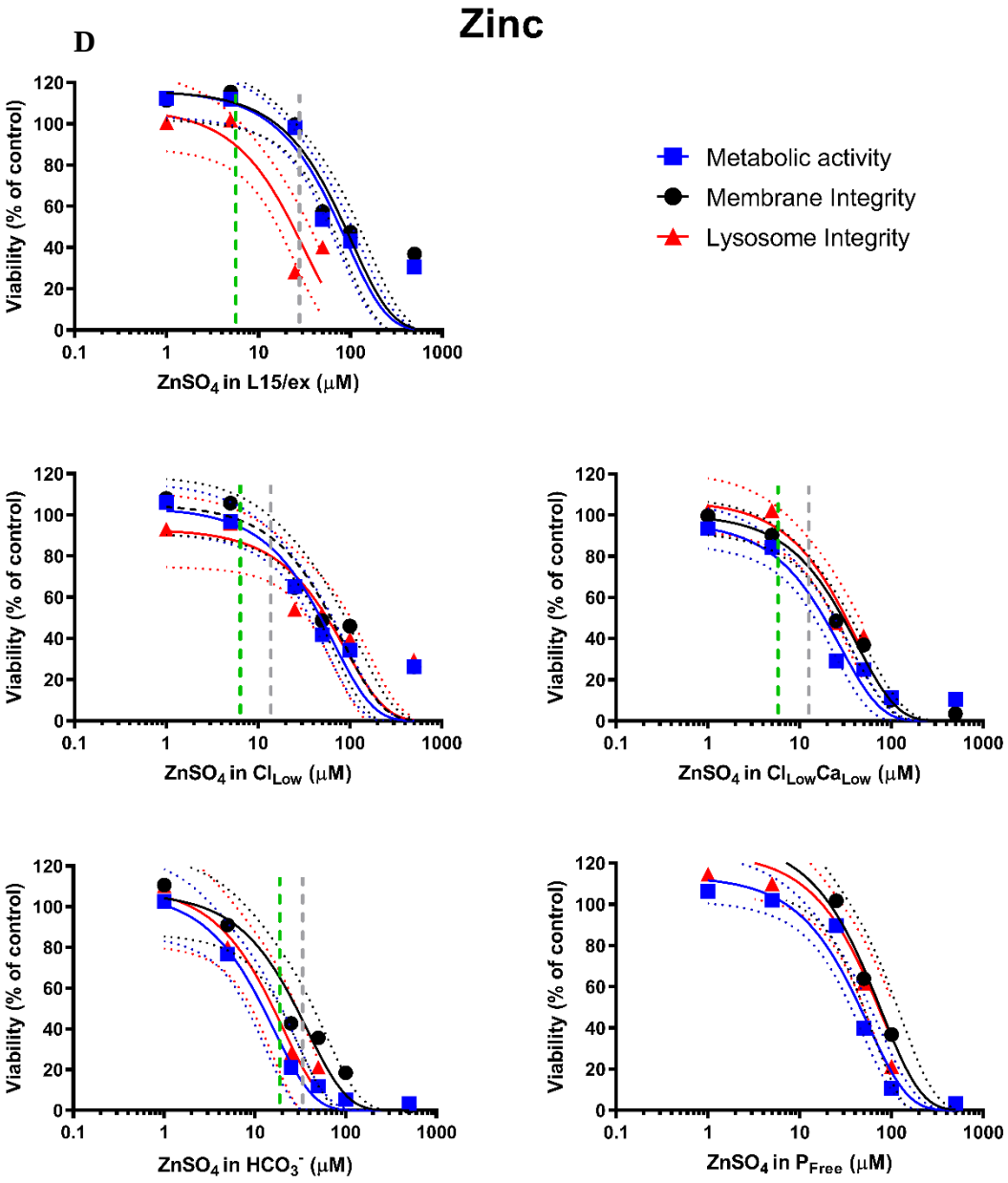

Figure 3D: Dose response curves for zinc toxicity in RTgutGC cell viability exposed to zinc for 24 hours in five different culture media differing in selected compontes (see Table 1). Viability is reported as percent of control (i.e. unexposed cells). Values shown are averages and dashed line represent 95% confidence interval of 3-12 independent experiments (n= 3-12). Solid lines represent the fitted curve. Vertical dashed lines show precipitation of metal (green = ~1% precipitation; grey = ~50% precipitation).

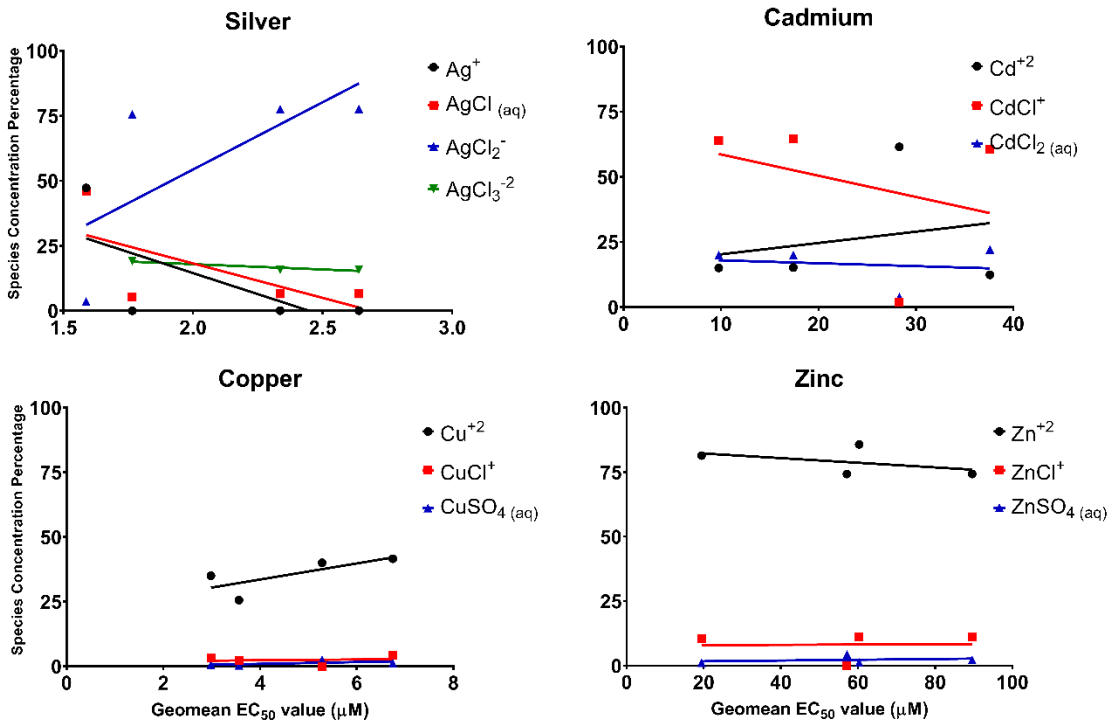

Figure 4: Correlation of metal speciation and geomean EC_{50} values. Geomean EC_{50} mean values were correlated with the calculated concentration of the specific metal species. Y axis represents species concentration percentage of total metal while the X axis is the EC_{50} values in µM. Species not found in at least 3 media were removed from the calculation, and L-15/Cl_{Low}-Ca_{Low} was removed due to Ca not effecting speciation. Correlation was calculated using the Pearson R correlation coefficients ($p < 0.05$; see Table 5).

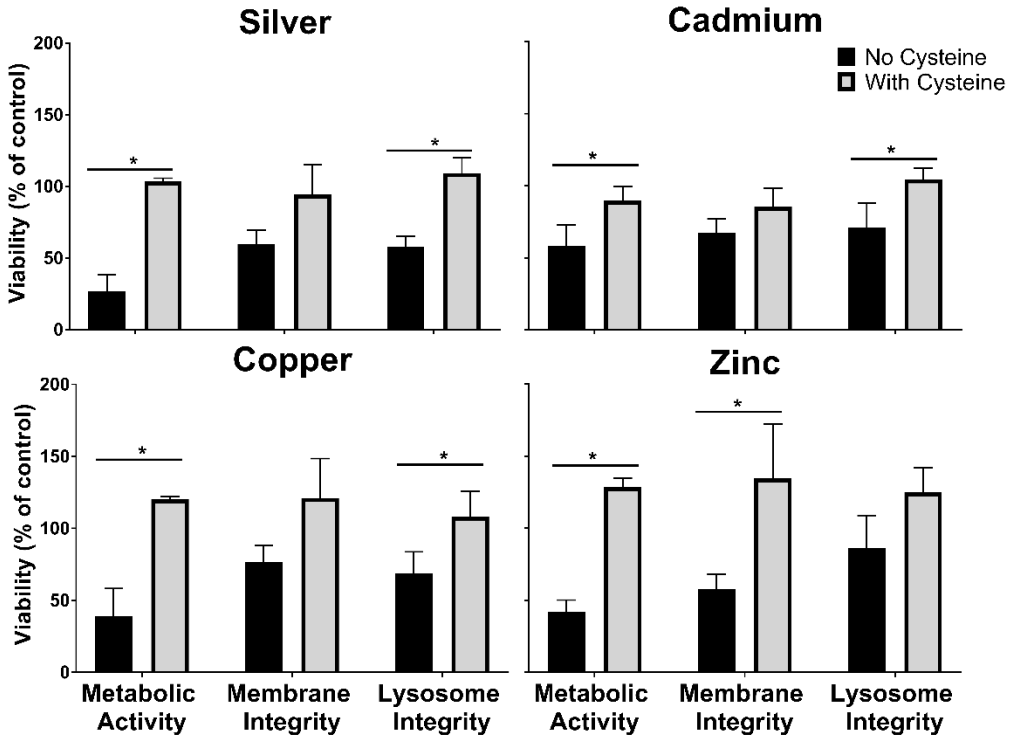

Figure 5: Protective effect of cysteine on metal toxicity in RTgutGC cells exposed to Ag: 1 µM, Cd: 20 µM, Cu: 5 µM, and Zn:100 µM for 24 hours in L-15/ex with (grey) and without (black) 500 µM L-cysteine. Values are mean ± standard deviation of three independent experiments, n=3. Asterisk indicates statistical difference between treatments (t-test, $p<0.05$).

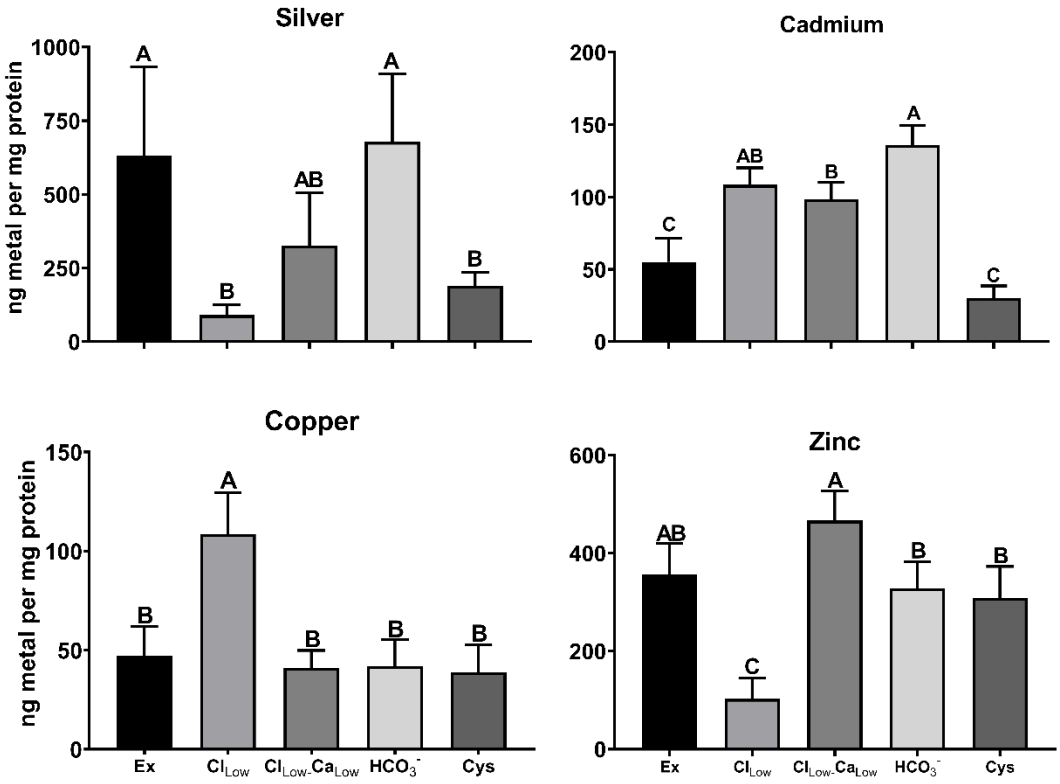

Figure 6: Metal bioavailability in RTgutGC cells measured by ICP-MS. RTgutGC were exposed for 24 hours to 0.6 µM of metal dissolved in the indicated media. Values are reported in ng of metal/mg of protein to account for variation in cell numbers. Values are mean ± SD of cells seeded in 4 different wells (n=4). Values bearing different letters are significantly different from each other (one-way ANOVA with a Tukey post-hoc test, $p < 0.05$, n=3-4).

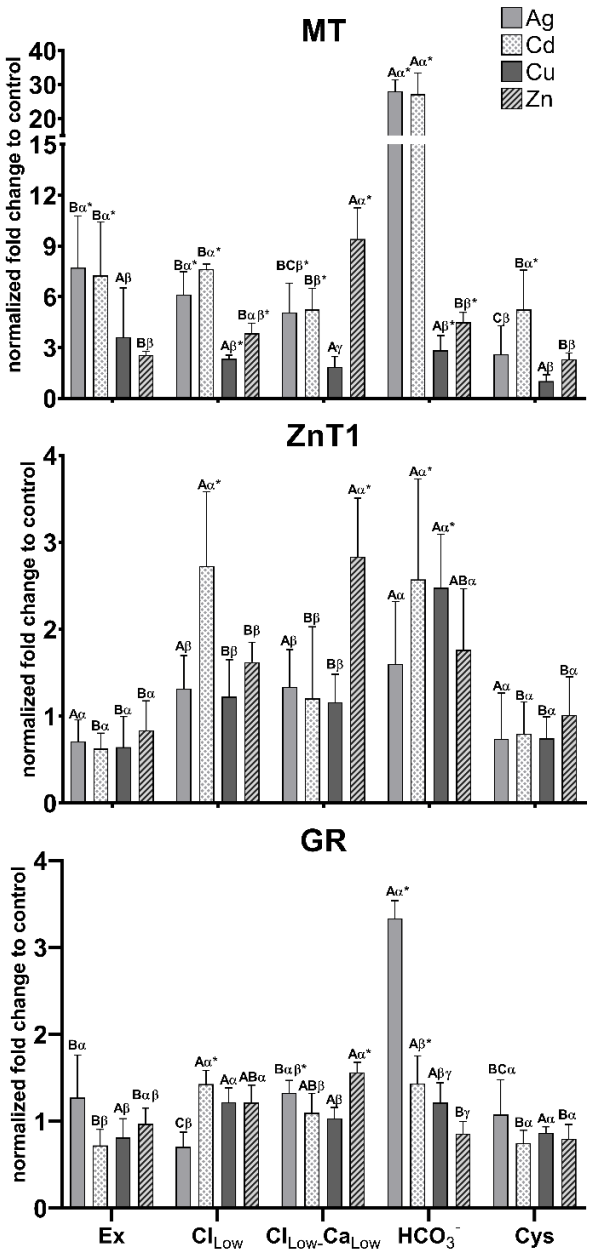

Figure 7: Glutathione Reductase, Metallothionine, and Zinc Transporter 1 mRNA levels (normalized fold change to controls) measured in RTgutGC exposed for 24 hours to 600 nM of metal in different media. Bars are mean ± SD of cells seeded in 5 different wells, n=5. Bars bearing different letters are statistically different within metal exposures (i.e. metal effect) and bars bearing different greek letters are statistically different within media conditions (i.e. media effect) (Two-way ANOVA, Tukey post hoc, $n \geq 3$, $p < 0.05$) and an asterisk represent statistical difference from the respective control (i.e. unexposed cells) ($p < 0.05$; One-way ANOVA, Dunnet post hoc, $n \geq 3$).

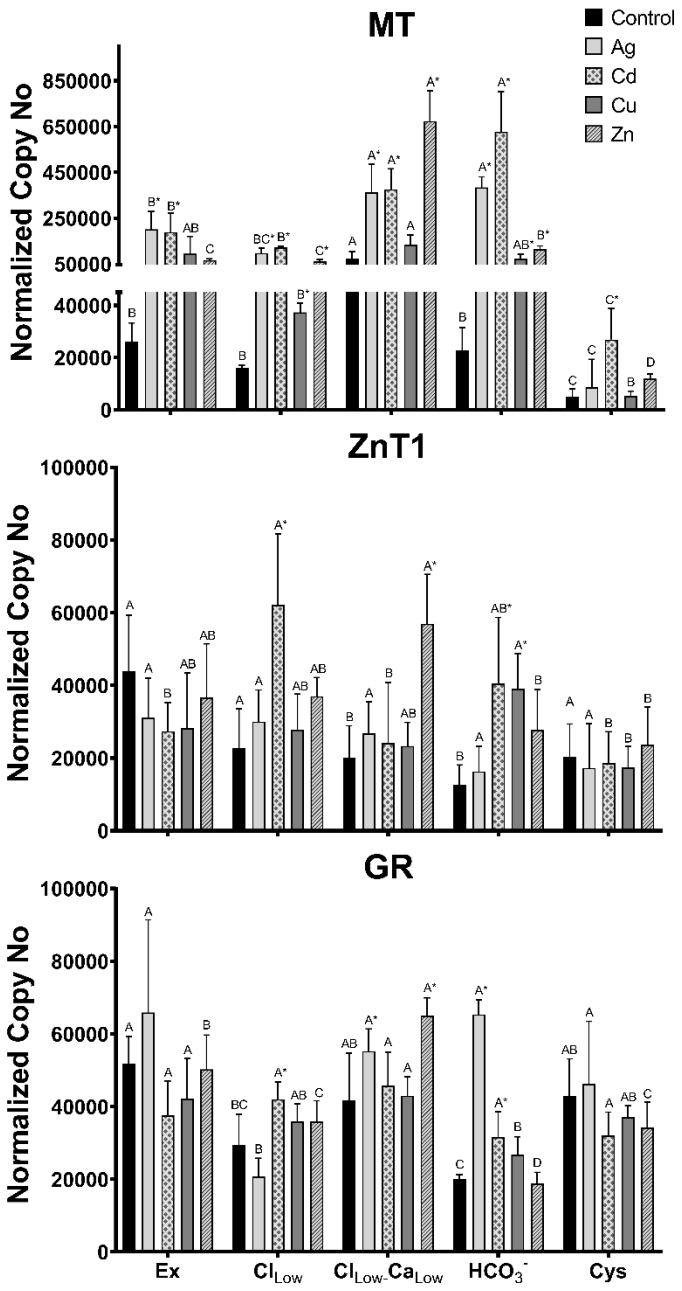

Figure 8: Normalized Glutathione Reductase, Metallothionine, and Zinc Transporter 1 mRNA copy numbers measured in RTgutGC exposed for 24 hours to 600 nM of metal in different media. Bars are mean ± SD. Bars bearing different letters are statistically different within metal exposures (One-way ANOVA, Tukey post hoc, $p < 0.05$; $n \geq 3$) and asterisk represents statistical difference from the control within a media group (One-way ANOVA, Dunnet post hoc, $p < 0.05$; $n \geq 3$).

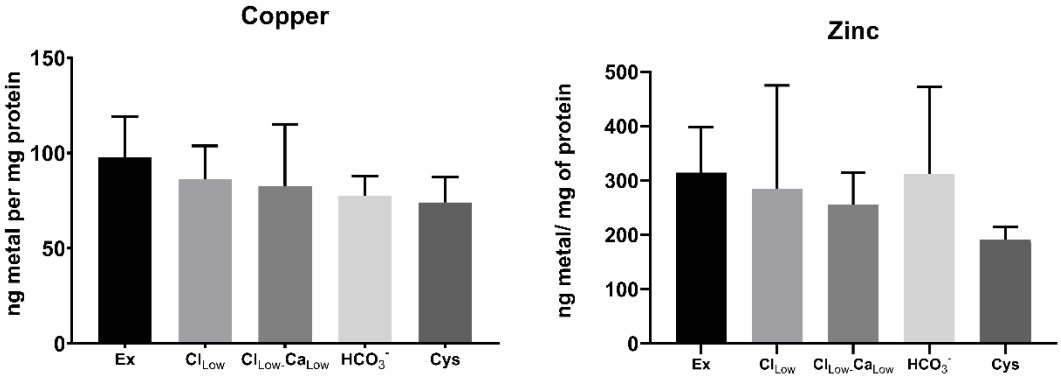

Figure 9: Mean ± SD concentrations of copper and zinc with in RTgutGC cells exposed to control media (without metal exposure) for 24 hours. Values represent ng of metal per mg protein. No statistical difference was found between media ($p>0.05$; One-way ANOVA, n=3-4).

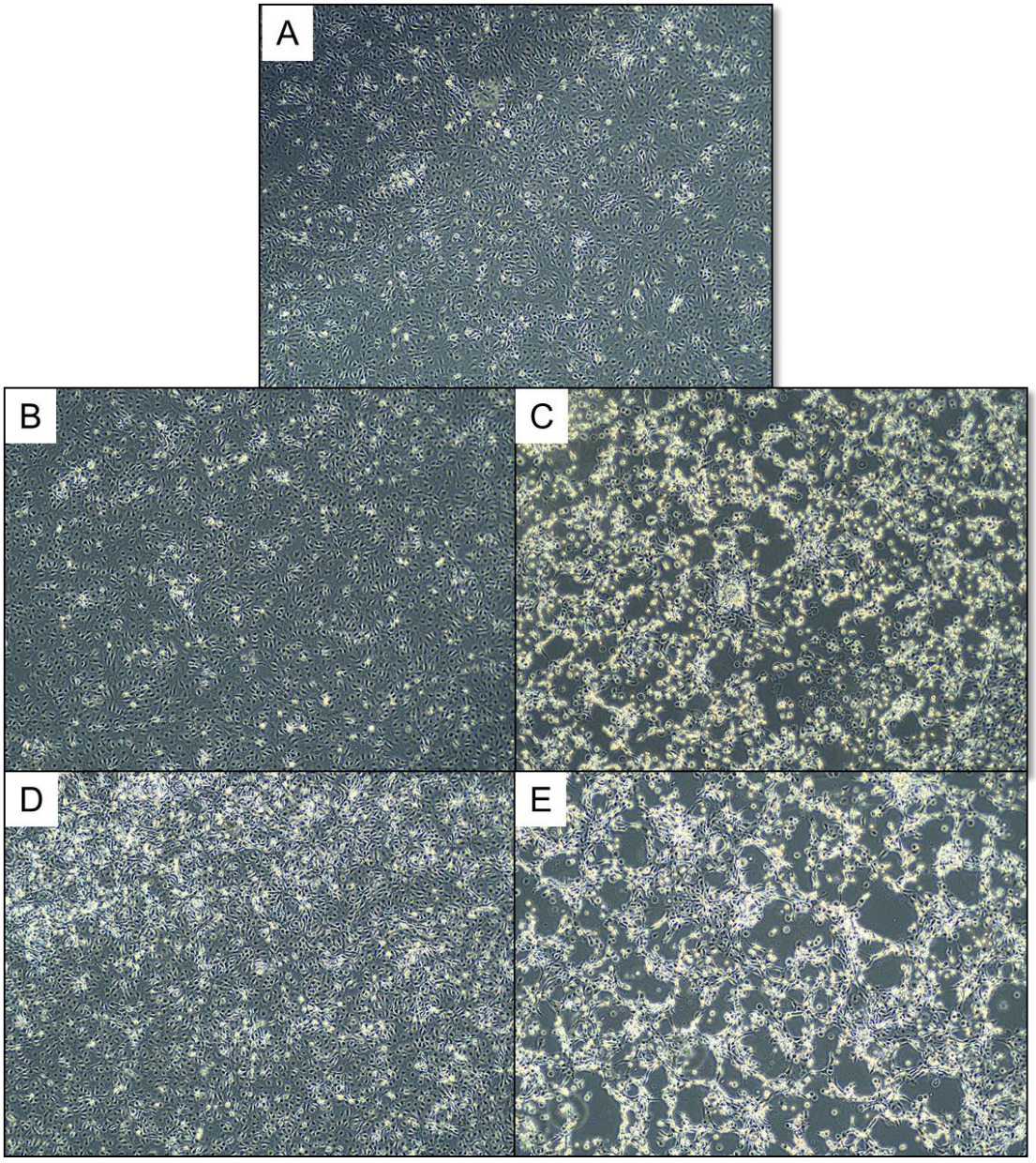

Figure 10: Images of cells exposed to metal free control media and 600 nM of silver in low chloride media. Cells exposed to 600 nM of $AgNO_3$ in L-15/ex (A), control L-15/Cl_{Low} (B) and control L-15/Cl_{Low}-Ca_{Low} (D) did not show noticeable characteristics of stress. Cells exposed to 600 nM $AgNO_3$ in 15/Cl_{Low} (C) and L-15/Cl_{Low}-Ca_{Low} (E), showed considerable stress such as cellular detachment from the well, vacuolization in the cells, and noticeably less cell density (cells per cm^2)

VITA

Dean Oldham

Candidate for the Degree of

Master of Science

Thesis: METAL SPECIATION'S ROLE IN TOXICITY, BIOAVAILABILITY, AND BIO-REACTIVITY IN THE RAINBOW TROUT (*ONCORHYNCHUS MYKISS*) GUT CELL LINE (RTGUTGC)

Major Field: Integrative Biology

Biographical:

Education:

Completed the requirements for the Master of Science in Integrative Biology at Oklahoma State University, Stillwater, Oklahoma in July 2020.

Completed the requirements for the Bachelor of SCIENCE IN Integrative Biology at Oklahoma State University, Stillwater, Oklahoma in 2018.

Completed the requirements for the Bachelor of Arts in History at Oklahoma State University, Stillwater, OK in 2013.

Experience:

Teaching Assistant: OSU, Stillwater, OK

Professional Memberships:

Society of Environmental Toxicology and Chemistry (SETAC)
OSU Graduate Society for Interdisciplinary Toxicology – ***Fellow 2020***
OSU Zoology Graduate Student Society (ZoGSS)